

Numerical analysis of the one-mode solutions in the Fermi-Pasta-Ulam system.

A. Cafarella, M. Leo and R.A. Leo

Dipartimento di Fisica dell'Università, 73100 Lecce, Italy,

Abstract

The stability of the one-mode nonlinear solutions of the Fermi-Pasta-Ulam - β system is numerically investigated. No external perturbation is considered for the one-mode exact analytical solutions, the only perturbation being that introduced by computational errors in numerical integration of motion equations. The threshold energy for the excitation of the other normal modes and the dynamics of this excitation are studied as a function of the parameter μ characterizing the nonlinearity, the energy density ϵ and the number N of particles of the system. The achieved results confirm in part previous results, obtained with a linear analysis of the problem of the stability, and clarify the dynamics by which the one-mode exchanges energy with the other modes with increasing energy density. In a range of energy density near the threshold value and for various values of the number of particles N , the nonlinear one-mode exchanges energy with the other linear modes for a very short time, immediately recovering all its initial energy. This sort of recurrence is very similar to Fermi recurrences, even if in the Fermi recurrences the energy of the initially excited mode changes continuously and only periodically recovers its initial value. A tentative explanation of this intermittent behaviour, in terms of Floquet's theorem, is proposed.

PACS numbers: 05.45.+b; 63.20.Ry; 63.10. + a

Keywords: Anharmonic lattices; Energy equipartition; Periodic solutions; Stability

1 Introduction

Since the computer experiment of Fermi-Pasta-Ulam (FPU) [1], many theoretical and numerical investigations followed to explain the unexpected results of the experiment [2] - [7]. What one expected according to a theorem of Poincarè [8] and a theorem proved by Fermi [9] himself in his youth, and what was instead observed, has been narrated in several papers (see e.g. [10]) in which various aspects of the experiment have been analysed in the framework of the KAM theorem [11], ergodic problem [12], statistical mechanics and chaotic behaviour of dynamical systems [13, 15].

It is well known [16, 17] that, for a periodic FPU- β chain with an even number of oscillators, an initial condition with only a set of excited modes, all having even (resp. odd) indices only, cannot lead to the excitation of modes having odd (resp. even) indices. This means that, if one considers the set of all modes partitioned in the two subsets of the even and odd modes, an initial excitation, completely contained in one of the two subsets, cannot propagate to the other.

There are also other partitions. For example, partitions exist for which a subset contains one mode only [18]. More specifically, for each of the modes

$$n = \frac{N}{4}; \quad \frac{N}{3}; \quad \frac{N}{2}; \quad \frac{2}{3}N; \quad \frac{3}{4}N, \quad (1)$$

(of course when N has the divisibility property required for n in (1) to be an integer) one has that, if only one of these mode is initially excited, it remains excited without transferring energy to any other mode.

An important problem is obviously the stability of these one mode solutions (OMS's), since it is reasonable to expect some relation between the loss of their stability and the onset of chaos in the system. In some sense, the destabilization of the simplest nonlinear modes can provide an "upper bound" estimate for the onset of the large scale chaos. The analysis of the stability of a generic OMS is very difficult from a mathematical point of view. Only for the case $n = N/2$ there are analytical results (see for example [19], [20], [18]) which estimate the threshold energy density for the mode to become unstable. In fact the mode $n = N/2$ is the simpler one, since the different components of the perturbation, in modal space, are all decoupled and are described by a single Lamé equation.

In this paper we numerically revisit the problem of stability of the OMS's and we present the results of a global analysis. We made a numerical study of the stability of the OMS's as a function of the number N of particles and of the product $\epsilon\mu$, where ϵ is the energy density and μ is the parameter of nonlinearity in the Hamiltonian of the system. The analysis is based on the numerical integration of the full nonlinear FPU model. No external perturbation is considered for the OMS, the only perturbation being that introduced by computational errors in numerical integration of motion equations. This simple method works very well: the results obtained confirm previous results obtained with a linear analysis of the problem of the stability([19], [20], [18]) and clarify the dynamics with which a nonlinear one-mode exchanges energy with the other linear modes, with increasing energy densities. We have found that, in a large range of initial excitation energy density, the energy of the OMS's keeps constant for very long times, and for short times it is partially transferred to other linear modes; furthermore the OMS's corresponding to the two values $n = \frac{N}{4}$ and $n = \frac{3}{4}N$ and the OMS's corresponding to $n = \frac{N}{3}$ and $n = \frac{2}{3}N$ have the same stability properties.

2 The FPU system

The FPU system is a one-dimensional chain of oscillators (with unit mass), with weakly non-linear nearest-neighbour interaction. The nonlinear forces considered are quadratic, cubic and broken linear ones. In the present work we consider only the FPU- β model (nonlinear cubic forces), with periodic boundary conditions. Calling q_n and p_n the coordinates and the momenta of the oscillators, the model is defined by the following Hamiltonian:

$$H = H_0 + H_1, \quad (2)$$

being

$$H_0 = \frac{1}{2} \sum_{k=1}^N p_k^2 + \frac{1}{2} \sum_{k=1}^N (q_{k+1} - q_k)^2, \quad (3)$$

$$H_1 = \frac{\mu}{4} \sum_{k=1}^N (q_{k+1} - q_k)^4, \quad (4)$$

with $q_{N+1} = q_1$.

If we introduce the normal coordinates Q_k and P_k of the normal modes through the relations:

$$Q_k = \sum_{j=1}^N S_{kj} q_j, \quad (5)$$

$$P_k = \sum_{j=1}^N S_{kj} p_j, \quad (6)$$

$$S_{kj} = \frac{1}{\sqrt{N}} \left(\sin \frac{2\pi k j}{N} + \cos \frac{2\pi k j}{N} \right), \quad (7)$$

the harmonic energy of mode k is:

$$E_k = \frac{1}{2} (P_k^2 + \omega_k^2 Q_k^2) \quad (8)$$

where, in the case of periodic boundary conditions,

$$\omega_k^2 = 4 \sin^2 \frac{\pi k}{N}. \quad (9)$$

We have $\omega_k = \omega_{N-k}$, so that there are only $\frac{N}{2}$ different frequencies (if we assume N even, for simplicity).

From (3 - 4), the Hamilton equations are obtained in the variables q_k and p_k , which, integrated by standard methods, allow to calculate the normal modes and the energy of each mode.

3 The one-mode solutions

Let us first consider the case $\mu = 0$. In this case all normal modes oscillate independently one from another and their energies E_k are constants of motion.

In the anharmonic case ($\mu \neq 0$), the normal modes are not independent and the variables Q_k have not simple sinusoidal oscillations. All the modes are coupled and the differential equation for the k -th mode is [18]:

$$\ddot{Q}_k = F_k(Q_1, \dots, Q_{N-1}), \quad (k = 1, \dots, N-1), \quad (10)$$

where F_k is the generalized force in normal coordinate space, given by:

$$F_k(Q_1, \dots, Q_{n-1}) = -\omega_k^2 Q_k - \frac{\mu\omega_k}{2N} \sum_{i,j,l}^{N-1} \omega_i\omega_j\omega_l C_{kijl} Q_i Q_j Q_l \quad (11)$$

and

$$C_{ijkl} = -\Delta_{i+j+k+l} + \Delta_{i+j-k-l} + \Delta_{i-j+k-l} + \Delta_{i-j-k+l}, \quad (12)$$

being $\Delta_k = (-1)^m$ for $k = mN$, if m is a positive integer, and $\Delta_k = 0$ otherwise.

The nonlinear one-mode solutions correspond to the values of n :

$$n = \frac{N}{4}; \quad \frac{N}{3}; \quad \frac{N}{2}; \quad \frac{2}{3}N; \quad \frac{3}{4}N. \quad (13)$$

From (11) and (12), one deduces [18] that, if only one of these modes is initially excited, it remains excited without transferring energy to any other mode. In this case, the equation of motion for the excited mode amplitude Q_n is:

$$\ddot{Q}_n = -\omega_n^2 Q_n - \frac{\mu\omega_n^4 C_{nnnn}}{2N} Q_n^3. \quad (14)$$

If we assume that at time $t = 0$ $Q_n \neq 0$ and $P_n = 0$, the solution of (14) is:

$$Q_n(t) = A \operatorname{cn}(\Omega_n t, k), \quad (15)$$

where Ω_n and the modulus k of the Jacobi elliptic function cn both depend on A:

$$\Omega_n = \omega_n \sqrt{1 + \delta_n A^2}, \quad (16)$$

$$k = \sqrt{\frac{\delta_n A^2}{2(1 + \delta_n A^2)}}, \quad (17)$$

with $\delta_n = \mu \epsilon C_{nnnn}/2N$.

The solution (15) is periodic with period $T_n = 4K(k)/\Omega_n$ where $K(k)$ is the complete elliptic integral of the first kind. The energy of the mode is:

$$E_n = \frac{1}{2} (P_n^2 + \omega_n^2 Q_n^2 + \mu \frac{\omega_n^4 Q_n^4 C_{nnnn}}{4N}). \quad (18)$$

In the next section, the problem of the stability of the OMS corresponding to $n = N/2$ will be analysed.

4 The stability of the one-mode solution $N/2$

The stability properties of the nonlinear mode $N/2$ was studied analytically some years ago. In [19], the nonlinear mode $N/2$ was named "the out of phase mode". This expression derives from the fact that from (5) and the properties of S_{kj} one has, if the only excited mode is the mode $N/2$:

$$q_k = \frac{1}{\sqrt{N}}(-1)^k Q_{N/2} \quad (19)$$

and then:

$$q_{k+1}(t) = -q_k(t), \quad k = 1, 2, \dots, N. \quad (20)$$

In [19], the stability analysis of the out of phase mode (mode $N/2$) starts from the equations of motion for the variables q_k . Due to the relations (20), these equations reduce to a single equation, describing the anharmonic oscillations of each particle, whose solution is the Jacobi elliptic cosine function. Perturbing this solution, and passing to normal modes variables Q_k one obtains a Lamé equation. The stability of the solutions of this equation, which is an example of Hill's equation, and then the stability of the mode $N/2$, is studied with the Floquet theory. A numerical analysis shows that the first mode which becomes unbounded, as energy density increases, is the mode $k = N/2 - 1$. A simple approximate formula, valid for large N and $\mu = 1$ and derived approximating the Hill's matrix with a 3×3 matrix, gives for the threshold energy density:

$$\epsilon_t = \frac{E_t}{N} = \frac{3.226}{N^2} + 0(N^{-4}). \quad (21)$$

The problem of stability of the mode $N/2$ was also tackled in [20], in connection with the study of tangent bifurcation of band edge plane waves in nonlinear Hamiltonian lattices. In the limit of large N , the formula

$$\epsilon_t = \frac{E_t}{N} = \frac{\pi^2}{3N^2} \approx \frac{3.29}{N^2} \quad (22)$$

is derived for the bifurcation energy density corresponding to the threshold energy density. This result is slightly different from the result (21) and the small difference is probably due to the rough estimate of the eigenvalue spectrum of the Hill's matrix in [19].

The problem of stability of a OMS was reconsidered subsequently in [18] with a detailed analysis of the mode $N/2$. This is the simpler case, because, as we have seen, the different components of the perturbation, in modal space, are all decoupled and can be reduced to the single Lamé equation:

$$\ddot{x}_r = -\omega_r^2 \left[1 + \frac{12 \mu A^2 cn^2(\Omega_{N/2} t; k)}{N} \right] x_r, \quad r = 1, \dots, N - 1. \quad (23)$$

To obtain in very simple way this equation, we observe that from (2), (3) and (4) one has:

$$\dot{p}_k = q_{k+1} + q_{k-1} - 2q_k + \mu[(q_{k+1} - q_k)^3 - (q_k - q_{k-1})^3]. \quad (24)$$

If the coordinates q_k are affected by some error, then the error on the \dot{p}_k , $\Delta \dot{p}_k$, will be:

$$\Delta \dot{p}_k = \Delta q_{k+1} + \Delta q_{k-1} - 2\Delta q_k + 3\mu[(q_{k+1} - q_k)^2(\Delta q_{k+1} - \Delta q_k) - (q_k - q_{k-1})^2(\Delta q_k - \Delta q_{k-1})]. \quad (25)$$

From (19) and (20) we have:

$$(q_{k+1} - q_k)^2 = (q_k - q_{k-1})^2 = \frac{4}{N} Q_{\frac{N}{2}}^2. \quad (26)$$

From (25) and (26) we obtain:

$$\Delta \dot{p}_k = \Delta q_{k+1} + \Delta q_{k-1} - 2\Delta q_k + \frac{12\mu}{N} Q_{\frac{N}{2}}^2 [\Delta q_{k+1} + \Delta q_{k-1} - 2\Delta q_k]. \quad (27)$$

Since $\Delta \dot{q}_k = \Delta p_k$, (27) reads:

$$\Delta \ddot{q}_k = [1 + \frac{12\mu}{N} Q_{\frac{N}{2}}^2] [\Delta q_{k+1} - 2\Delta q_k + \Delta q_{k-1}]. \quad (28)$$

Passing to modal variables Q_k , we finally have:

$$\Delta \ddot{Q}_k = -\omega_k^2 [1 + \frac{12\mu}{N} Q_{\frac{N}{2}}^2] \Delta Q_k, \quad (29)$$

which is equation (23).

We want to remark, however, that eq. (29) (and then (23)), on which is based the study of the stability reported in [18], is the result of a linear analysis and consequently all its implications have only local value.

We outline now the stability analysis of the one-mode $N/2$, given in [18]. Let be k the modulus of the Jacobian elliptic functions. It is related to the product $\beta = \epsilon\mu$ by the relation:

$$\beta = \frac{k^2}{1 - 2k^2} (1 + \frac{k^2}{1 - 2k^2}). \quad (30)$$

Expressing $\Omega_{N/2}$ and $\mu A^2/N$, as functions of k , and after rescaling time at each fixed k , each of the Lamé equations (23) can be put in the standard form:

$$y'' + [\alpha - \nu(\nu + 1) k^2 \operatorname{sn}^2(u, k)] y = 0, \quad (31)$$

where the prime superscript denotes differentiation with respect to the new time $u = \Omega_{N/2} t$, y stands for the generic variable x_r and the parameters α and ν are defined by the relations:

$$\alpha = \frac{1}{4}(1 + 4k^2)\omega_r^2, \quad \nu(\nu + 1) = \frac{3}{2}\omega^2.$$

Putting:

$$\rho = \sin^2(\pi r/N), \quad (32)$$

the two last relations become:

$$\alpha = \rho(1 + 4k^2), \quad \nu(\nu + 1) = 6\rho.$$

A given pair (ρ, k) describes different mode numbers r in systems with different N , all having the same r/N value, with the same value of the product $\beta = \epsilon\mu$ for the unperturbed solution $n = N/2$. To solve the stability problem for generic values of ν , the equation (31) is reduced to a Mathieu equation, by approximating the sn^2 by its first-order Fourier expansion. After a further time rescaling $\tau = \pi t'/2 K$, where K is the complete elliptic integral of the first kind, with modulus k , one obtains the canonical form of Mathieu equation:

$$\frac{d^2 y}{d\tau^2} + [a - 2q \cos(2\tau)] y = 0, \quad (33)$$

where:

$$a = \rho \left(\frac{2K}{\pi} \right)^2 \left(-5 + 4k^2 + 6 \frac{E}{K} \right), \quad (34)$$

$$q = - \frac{12 \rho}{\sinh(\pi K'/K)}, \quad (35)$$

$$K'(k) = K \sqrt{1 - k^2}, \quad (36)$$

and E is the complete elliptic integral of the second kind, with modulus k . Both parameters a and q depend on k^2 and ρ . For each fixed ρ , which corresponds to fix a ratio r/N , changing k^2 , namely β , one can trace a curve in the (q, a) parameter plane. A stability transition happens if this curve intersects characteristic curves separating stable from unstable regions for the Mathieu equation.

The main results of the stability analysis reported in [18] are:

a) for each mode having $\rho > 1/3$, there is a threshold value of β for instability. Above this threshold the nonlinear mode $n = N/2$ presents an instability causing growth of the mode corresponding to ρ , through parametric resonance;

b) on the contrary, modes with $\rho < 1/3$ (i.e. $r/N < 0.196$) are always stable in the linear approximation, for any energy density of mode $n = N/2$, so that, perturbations of this mode involving only modes with $\rho < 1/3$ never lead to instability. These modes, as well as modes with $\rho > 1/3$, when the product $\epsilon\mu$ is less than the critical value, can grow only if they are triggered by the interaction with other modes that are unstable;

c) for $N \geq 4$ there are always modes with $\rho > 1/3$ so that the mode $N/2$ can never be stable for all energy densities. Since the threshold value of β is a decreasing function of ρ , the first modes to go unstable, when $\epsilon\mu$ is increased from zero, are the modes $r = N/2 - 1$ and $r = N/2 + 1$, which have $\rho = \cos^2(\pi/N)$. Therefore, for each (even) number N of particles, there is a non-zero value of β , function of N , below which the nonlinear mode $N/2$ is stable. Since the critical value tends to zero for $\rho \rightarrow 1$, the critical threshold for the stability approaches zero as the number N of particles is increased without limit;

d) using power series expansion of the various previous formulas, one obtains, for the critical value of threshold, the formula:

$$\beta_t = \frac{\pi^2}{3N^2} + 0(N^{-4}), \quad (37)$$

which confirms the N^{-2} dependence found in [19] and in [20] and the numerical values $\pi^2/3$ of the coefficient of $1/N^2$ found in [20].

5 Numerical results for the case $N/2$

In this section, we present the results of our numerical analysis of the stability of the one-mode solution corresponding to $n = N/2$, as a function of the product $\epsilon\mu$ and of the number N of particles, based on the numerical integration of the full nonlinear FPU model directly in the variables q_k, p_k . More precisely, we integrate the equations of motion in the variables q_k, p_k by means of a bilinear symplectic algorithm of the third order, which has been adapted from an algorithm employed previously by Casetti [21]. Initial conditions for the variables q_k, p_k are obtained in the following way. We excite the OMS, at $t = 0$, always putting $Q_{N/2} \neq 0$ and $P_{N/2} = 0$. In all the numerical experiments we fix $\mu = 0.1$ and change the value of the energy density $\epsilon = E_{N/2}/N$ where

$$E_{N/2} = \frac{1}{2}(P_{N/2}^2 + \omega_{N/2}^2 Q_{N/2}^2 + \mu \frac{\omega_{N/2}^4 Q_{N/2}^4}{2N}) \quad (38)$$

is the energy of the nonlinear one-mode $N/2$. If we fix the initial value of $E_{N/2}$ (or equivalently ϵ), the initial value of $Q_{N/2}$ is obtained from (38) with $P_{N/2} = 0$. Finally, from inverse transformations of (5) and (6), the values of $q_k(0)$ and $p_k(0)$ are obtained.

The normal coordinates $Q_{N/2}$ and $P_{N/2}$ of the nonlinear one-mode and the normal coordinates Q_k and P_k of the other normal modes are calculated at fixed time intervals, multiple of the integration step. Then, the study of the stability of the OMS is made through the analysis of both the time evolution of $Q_{N/2}$ and $P_{N/2}$ and the evolution of the other modes Q_k, P_k which are generated through computational errors.

As concerns the numerical integration, we use values of integration time steps Δt ranging from 0.01 to 0.005. For example, the first value is approximately $1/300$ of the smallest period of oscillation of the atoms in the harmonic case and allows us to obtain a control of the total energy E of the lattice, which ensures a relative error $\Delta E/E < 10^{-6}$.

To illustrate the various steps of our method of numerical analysis, let us consider the case $N = 32$ and thus the OMS $N/2 = 16$. In this case $C_{nnnn} = 2$ and we have the formula (38) for the energy of the nonlinear mode. We take a value of the energy density ϵ and integrate the equations of motion for the variables q_k and p_k . The integration time is fixed in such a way to observe the instability of nonlinear mode, if the value of $\beta = \epsilon\mu$ is greater than the theoretical value (37) of the threshold energy density. Typical values of this time are of order $10^6 \Delta t$ where Δt is the integration step.

For $N = 32$, we have $\beta_t = \pi^2/3N^2 = 0.00321$. We consider three values of β : the first one, $\beta = 0.001$, smaller than β_t , the second one, $\beta = 0.005$, larger and the third, $\beta = 0.1$, much larger than β_t . In Figs. 1 - 3, the behaviours of the nonlinear mode in the plane Q_{16}, P_{16} are shown for these three values of β , while in Figs. 4 - 6 we show $Q_{16}(t)$, as a function of time for the same values of β .

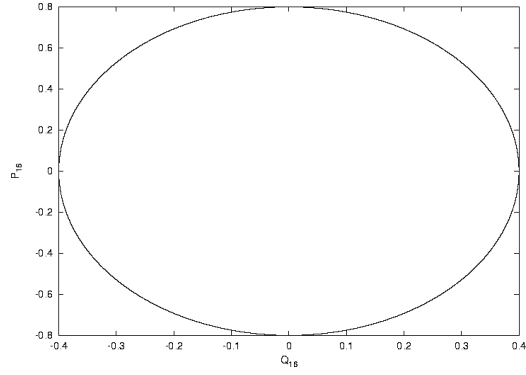


Figure 1: P_{16} vs Q_{16} for $\epsilon\mu = 0.001$

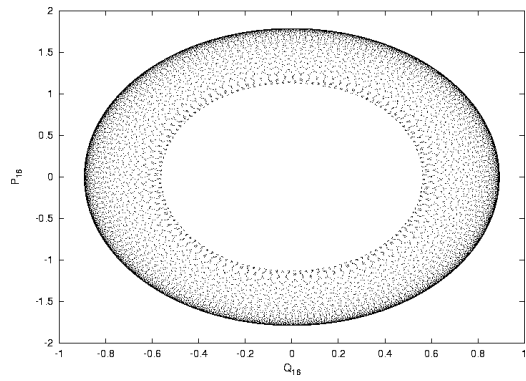


Figure 2: P_{16} vs Q_{16} for $\epsilon\mu = 0.005$

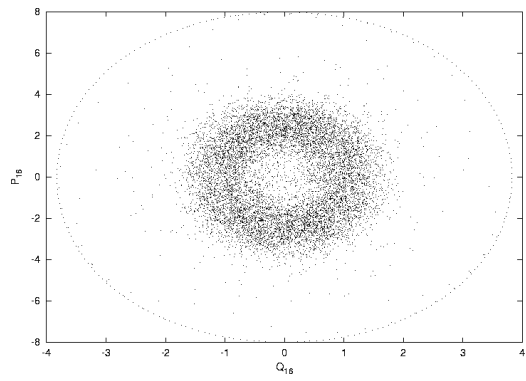


Figure 3: P_{16} vs Q_{16} for $\epsilon\mu = 0.1$

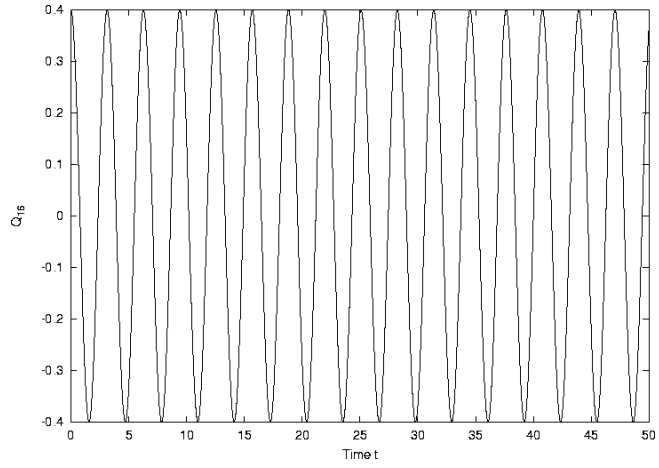


Figure 4: Q_{16} vs t for $\epsilon\mu = 0.001$

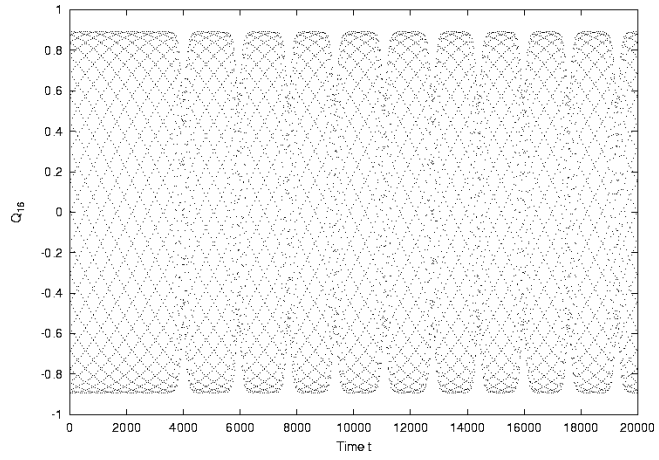


Figure 5: Q_{16} vs t for $\epsilon\mu = 0.005$

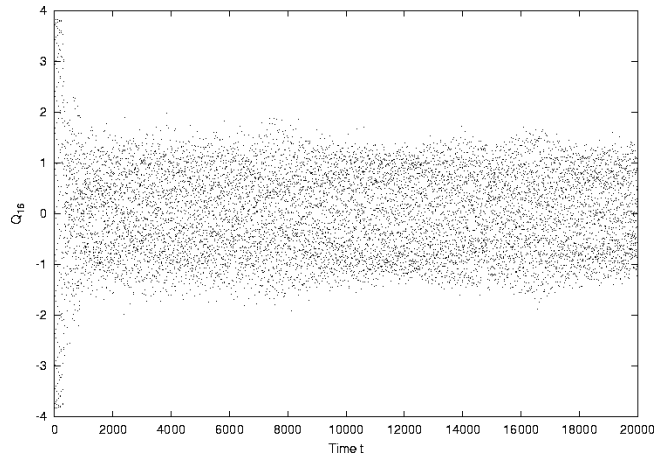


Figure 6: Q_{16} vs t for $\epsilon\mu = 0.1$

From the inspection of previous figures, we can observe that, for $\beta = \epsilon\mu$ very small, well below the threshold energy density, the nonlinear OMS $N/2$ is stable and Q_{16} is a periodic function with the same amplitude and the same period of the analytical solution. For $\epsilon\mu = 0.005$, above the threshold, the situation is very different. The period of oscillation is equal to the period of the analytical solution, and for very long times, in the plane Q_{16}, P_{16} , the representative point moves on a one-nonlinear dimensional closed curve, as for values of $\epsilon\mu$ very small; but now, periodically and for short times, the amplitude of oscillation varies, due to a decrease of modal energy, and the representative point of the system moves on an open curve which tends periodically to shrink. For $\epsilon\mu = 0.1$, well above the threshold energy density, we observe a chaotic behaviour. This behaviour is also evident from the inspection of the figures 7 - 9 in which the modal energy is shown, as a function of time, for the three values of β . In these figures, and in all the next figures which show the behaviour of energy vs time, the energy is always normalized to the initial excitation energy.

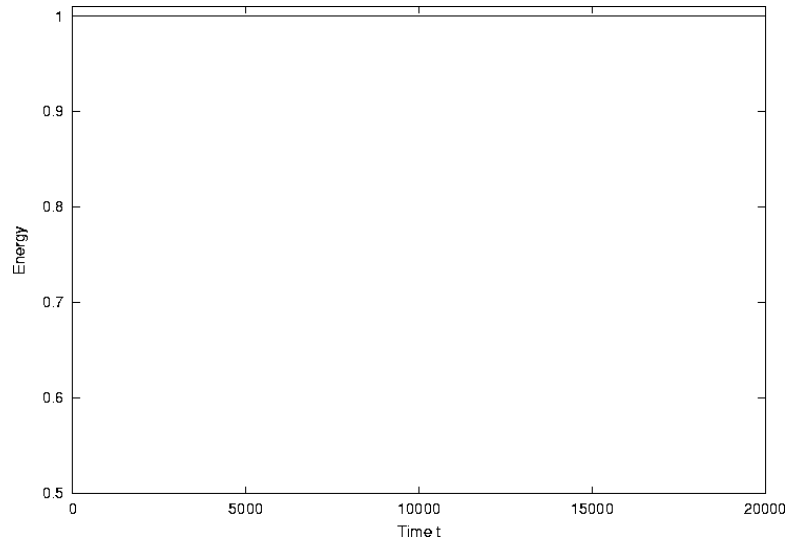


Figure 7: Energy of the mode 16 vs t for $\epsilon\mu = 0.001$

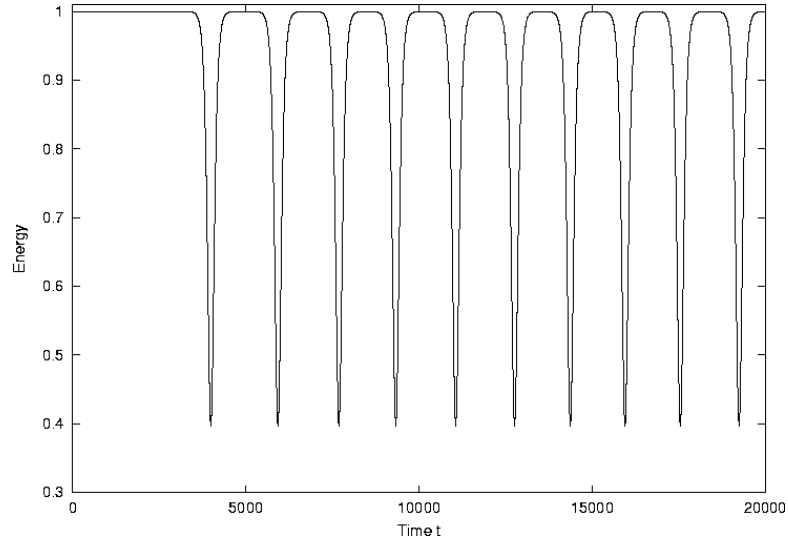


Figure 8: Energy of the mode 16 vs t for $\epsilon\mu = 0.005$

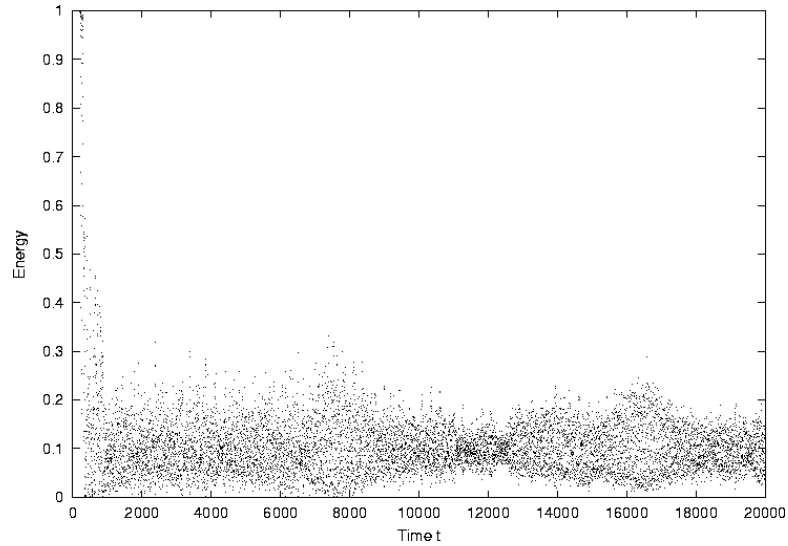


Figure 9: Energy of the mode 16 vs t for $\epsilon\mu = 0.1$

As can be seen from the last figures, it is evident that the mode 16 exchanges energy with some other mode. According to the theory developed in [19] and in [18], for $\beta = 0.005$, we are above the threshold for the excitation of the adjacent mode 15, which is the first to be excited, and the excitation of this mode, due to nonlinear coupling between the modes, should trigger other linear modes. In the figures 10 and 11 the behaviour of the the adjacent mode 15 is shown.

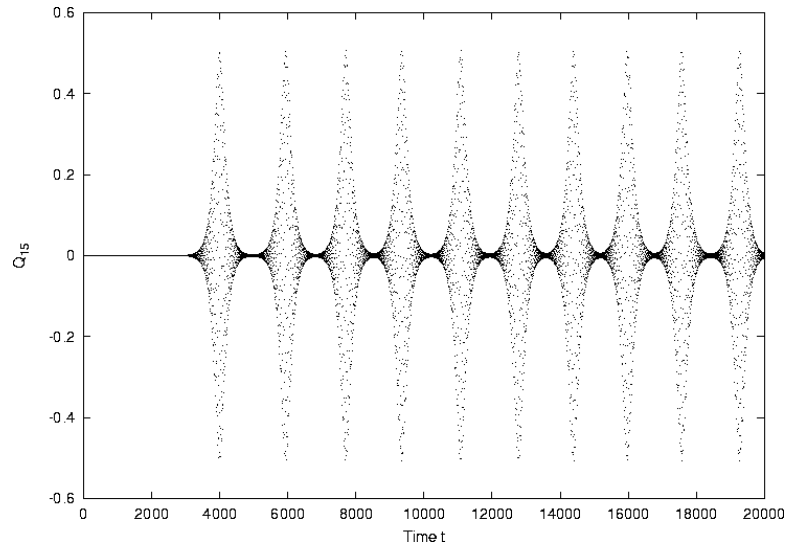


Figure 10: Q_{15} vs t for $\epsilon\mu = 0.005$

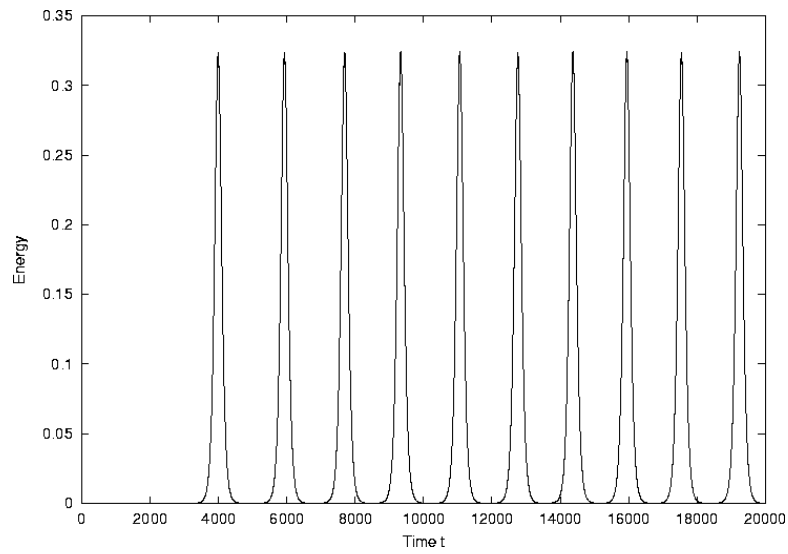


Figure 11: Energy of the mode 15 vs t for $\epsilon\mu = 0.005$

The contemporary excitation of the other modes is shown in Figs. 12 - 14, where the energies of the modes $n = N/2$, $n = 15$, $n = 14$ are shown, as functions of time. We remark that the energy of the mode 16 is calculated with the formula (18), while, for the other modes, the usual formula (8) is utilized. Of course, formula (8) is only indicative for large excitation energy, when the variables Q_k and P_k lose their meaning of modal variables.

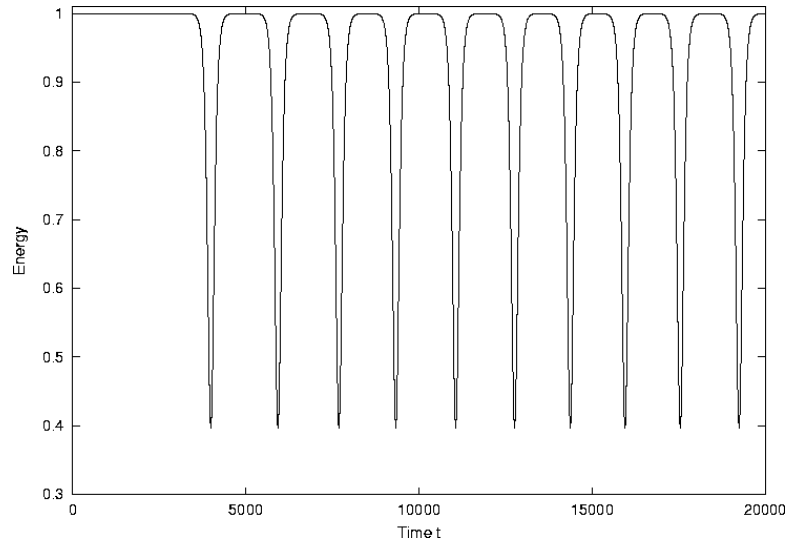


Figure 12: Energy of the mode 16 vs t for $\epsilon\mu = 0.005$

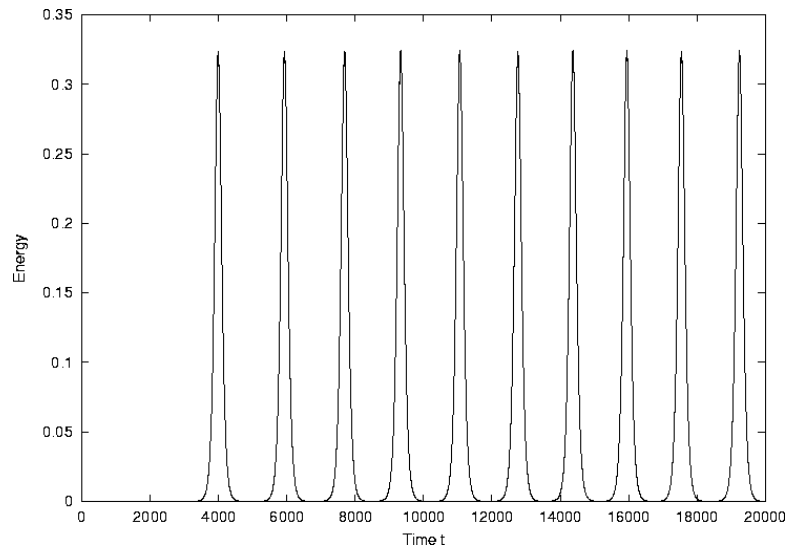


Figure 13: Energy of the mode 15 vs t for $\epsilon\mu = 0.005$

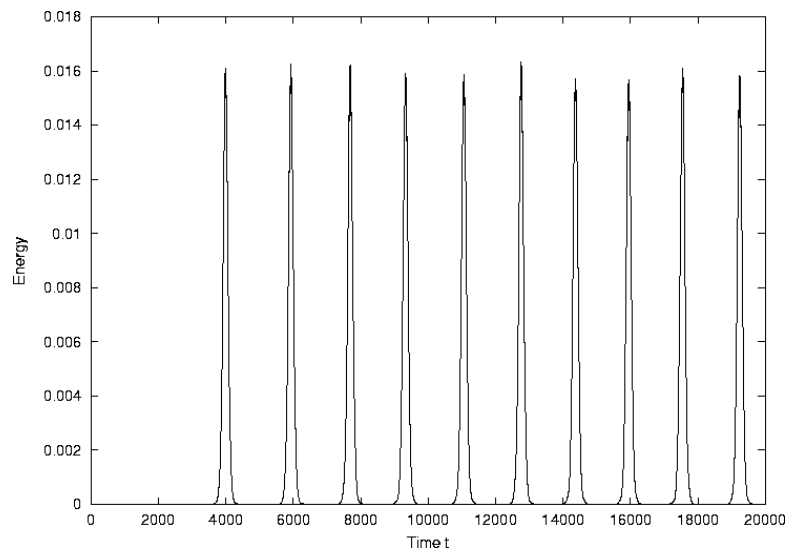


Figure 14: Energy of the mode 14 vs t for $\epsilon\mu = 0.005$

The first energy pulse, for the mode 15, appears as in Fig. 15. Near the maximum, the value of energy oscillates as in Fig. 16 with a period $T \approx \pi/2$, equal to half the period of the oscillations of Q_{16} .

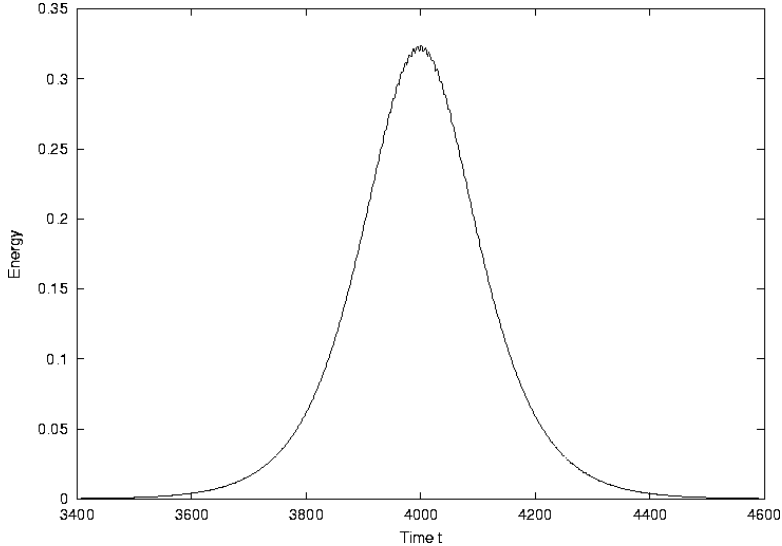


Figure 15: Behaviour of the energy of the mode 15 vs t for $\epsilon\mu = 0.005$

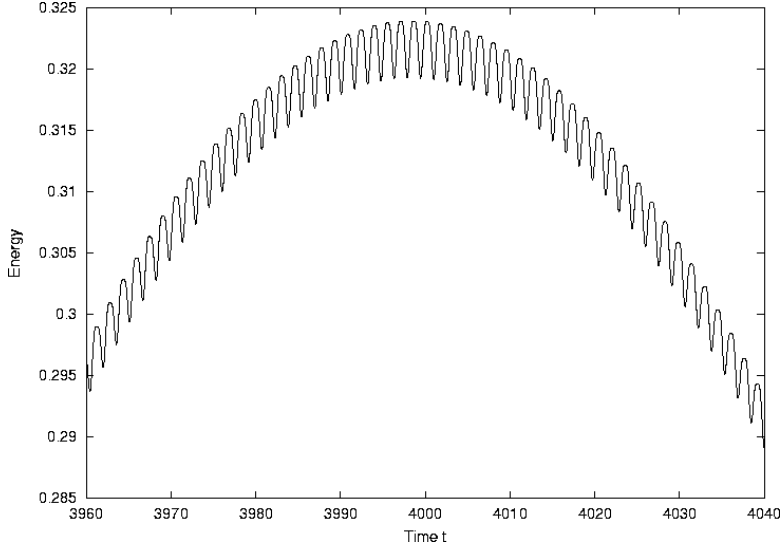


Figure 16: Behaviour of the energy of the mode 15 vs t for $\epsilon\mu = 0.005$, near the maximum

The initial time interval, necessary to excite, through computational errors, the other modes, depends obviously, on the precision of numerical computations. All the previous numerical calculations have been performed in double precision. We have observed that, working in simple precision, the exchange of energy of the mode $N/2$ with the other modes occurs much before than in double precision. However, since the mechanism is primed, it repeats with the same properties either in double or in simple precision.

The instability of the OMS can also be seen from another point of view, by considering the hamiltonian variables q_k . We recall that, if the OMS $Q_{N/2}$ were stable then, from (20), the sum $q_k + q_{k+1}$ would be always zero. In Fig. 17, as an example, we report the sum $q_{15} + q_{16}$ as a function of time. As can be seen from the figure, the instability (sum of the two coordinates different from zero) appears when the mode 16 starts to exchange energy with the other modes.

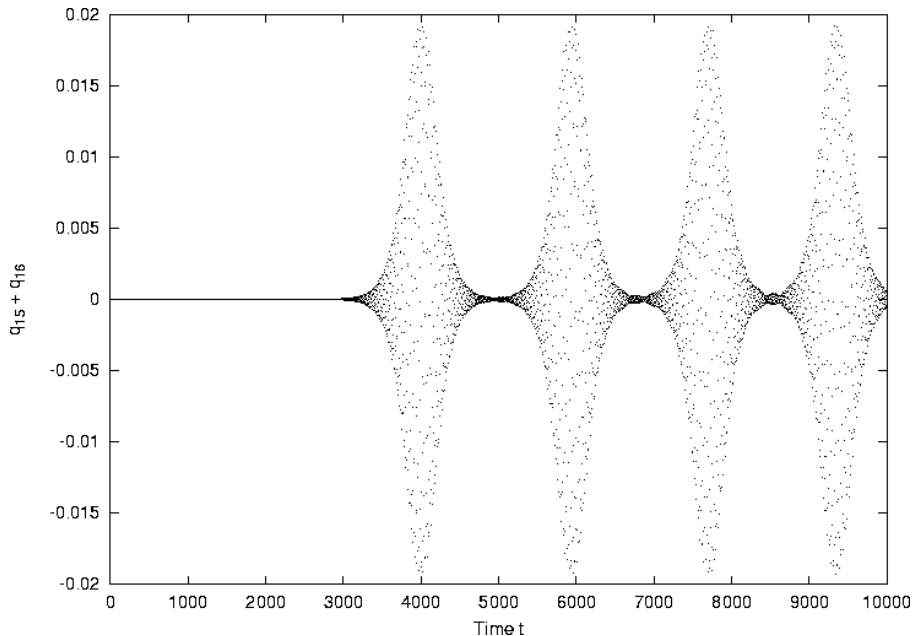


Figure 17: $q_{15} + q_{16}$ vs t for $\epsilon\mu = 0.005$ when the mode 16 is initially excited.

In this context, and to obtain more insight in the behaviour of OMS, it is really very interesting to see what are the positions of particles in the chain, i.e. the spatial configuration of the chain, in correspondence of a well determined value of energy of the OMS. In figs 18 - 23 for $\epsilon\mu = 0.005$, the values of the coordinates of the 32 atoms, in correspondence of a particular value of the energy of mode 16, are shown. To be clear, the representative points of the particles are joined by segments.

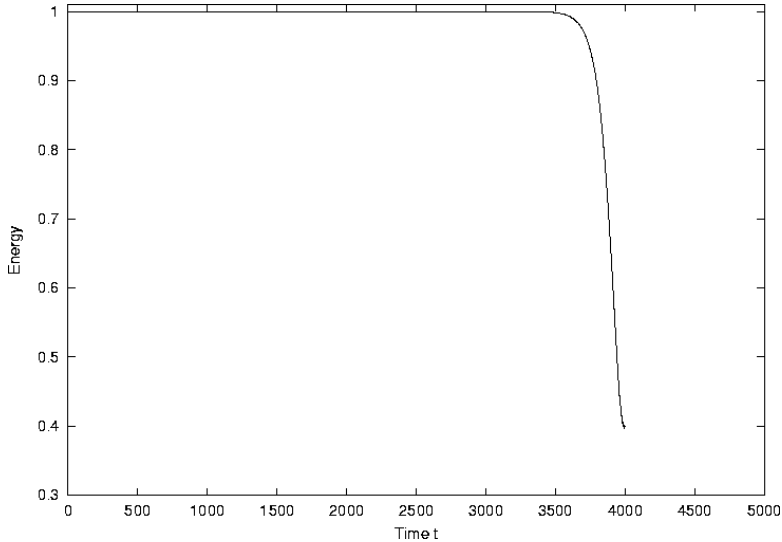


Figure 18: Energy of the mode 16 vs t for $\epsilon\mu = 0.005$

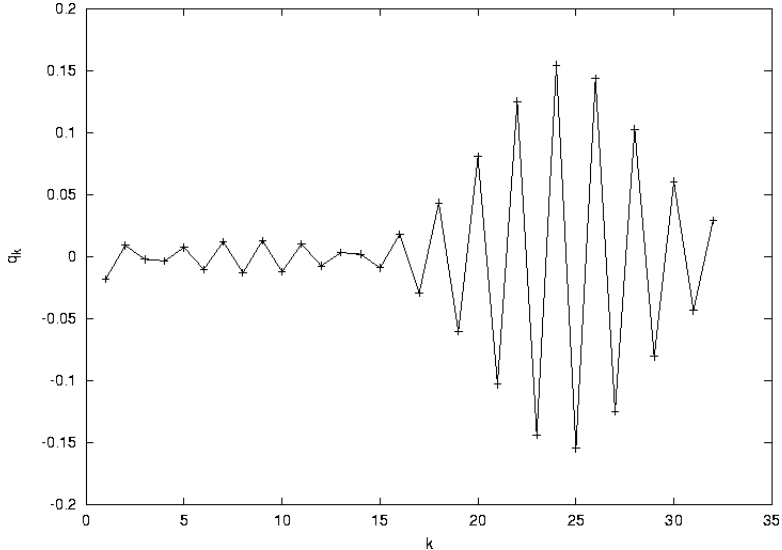


Figure 19: Values of the displacements of atoms in correspondence of the final value of energy in Fig. 18

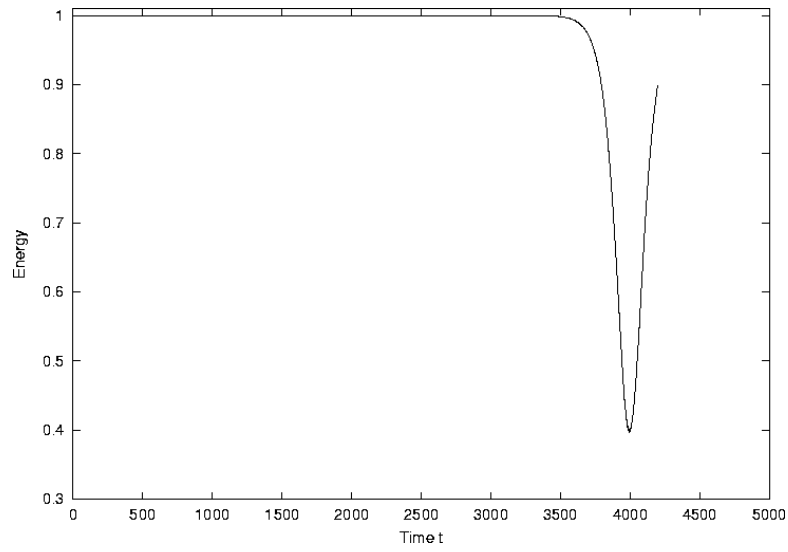


Figure 20: Energy of the mode 16 vs t for $\epsilon\mu = 0.005$

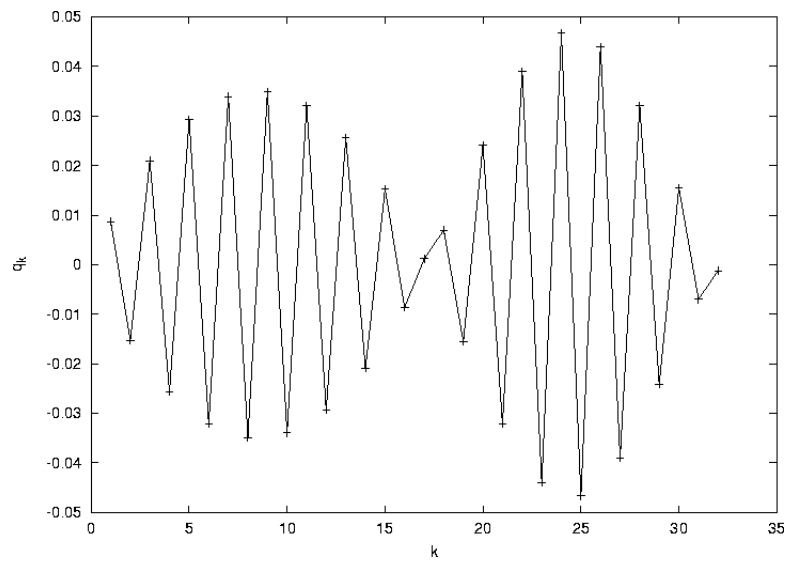


Figure 21: Values of the displacements of atoms in correspondence of the final value of energy in Fig. 20

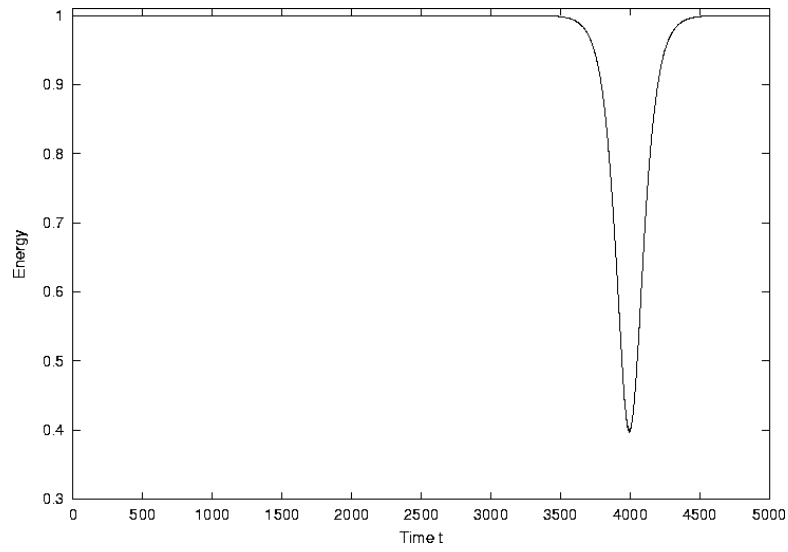


Figure 22: Energy of the mode 16 vs t for $\epsilon\mu = 0.005$

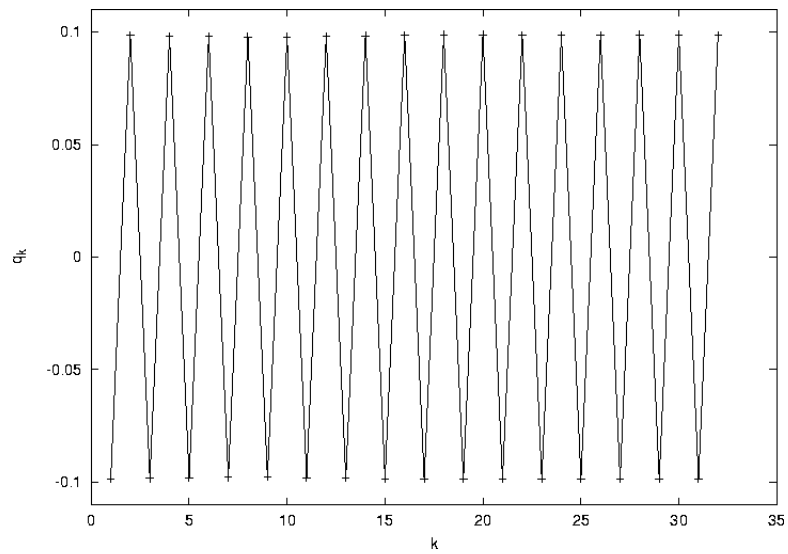


Figure 23: Values of the displacements of atoms in correspondence of the final value of energy in Fig. 22

As can be seen from the previous figures, the particle chain recovers its "symmetrical form" ($q_k + q_{k-1} = 0$) when the OMS recovers all its initial energy.

6 The case $N/2$ as a function of N

To complete the analysis of the case $N/2$, in the next figures we show the behaviour of the energy of this mode as a function of time for $N = 26, 38, 52$ and 54 , for $\epsilon\mu = 0.005$.

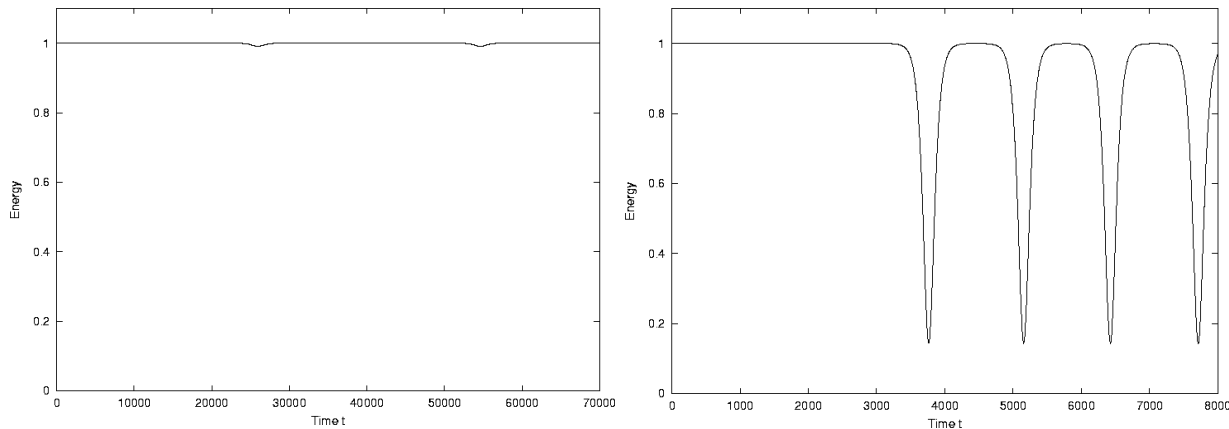


Figure 24: Energy of the mode $N/2$ vs t for $N = 26$ e $N = 38$.

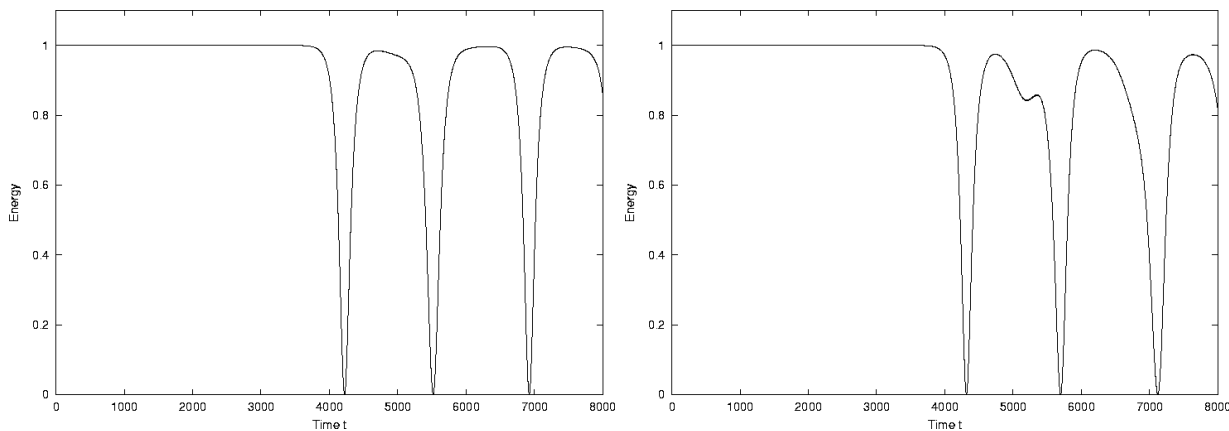


Figure 25: Energy of the mode $N/2$ vs t for $N = 52$ e $N = 54$.

From the previous figures it emerges that, increasing N , the mode $N/2$ tends to exchange all its energy. For $N = 52$, the mode $N/2$ periodically loses and recovers roughly all its energy. For $N > 52$, the recovery is not complete and moreover the curve of energy versus time becomes irregular. The irregularity and complexity of the curve increase with N and, for N very large, the system becomes chaotic. This behaviour is evident in the Figs. 26 and 27, which show the behaviour of the energy of the mode $N/2$, for $N = 256$ and $N = 512$.

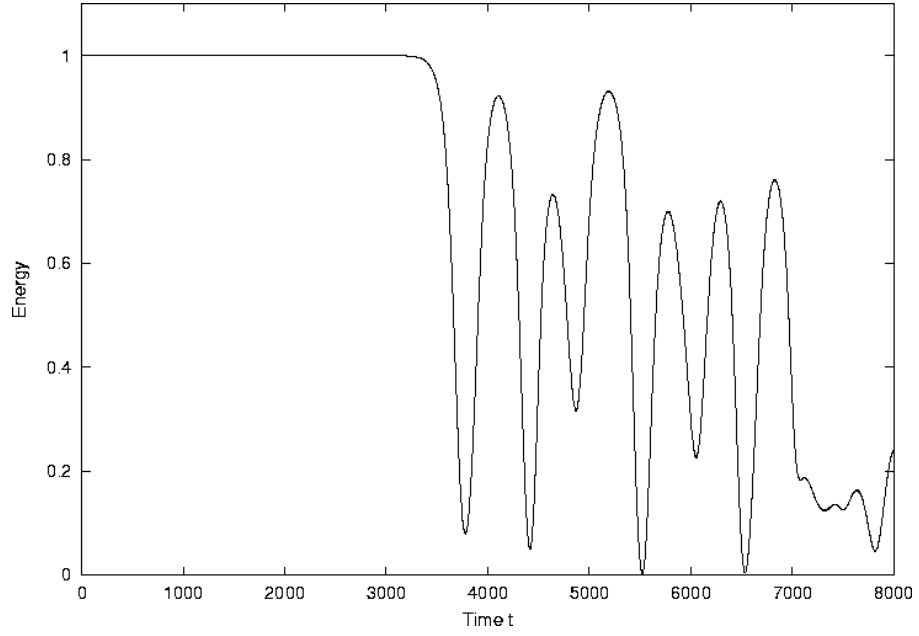


Figure 26: Energy of the mode 128 for $N = 256$ and $\epsilon\mu = 0.005$

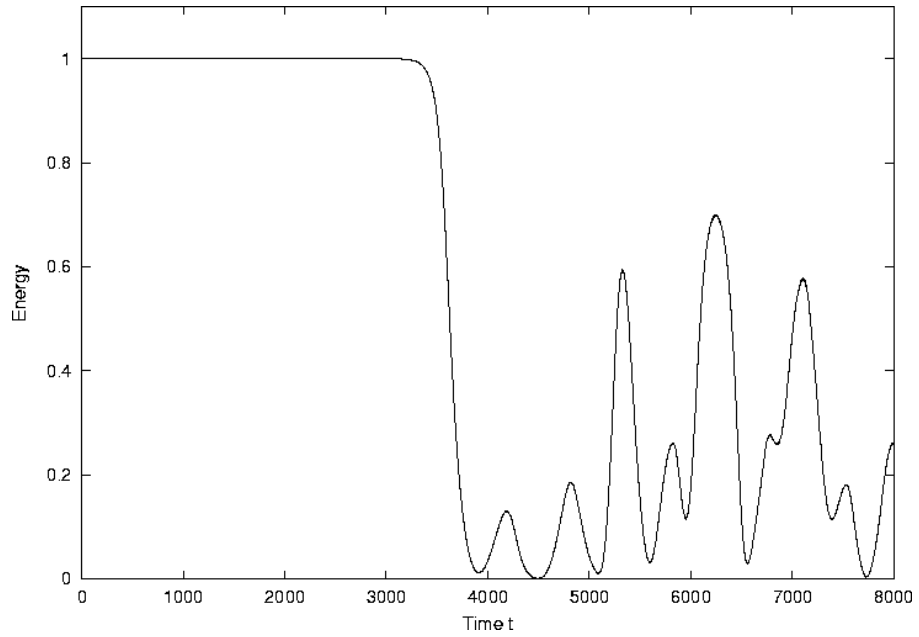


Figure 27: Energy of the mode 256 for $N = 512$ and $\epsilon\mu = 0.005$

Let us now consider the formula (37), obtained analytically, and let us see how we can obtain numerically the dependence on N of the threshold energy density. From the analysis of the stability reported in [19] and in [18], we know that the first modes to be excited, as the energy increases and the mode $N/2$ becomes unstable, are the modes $N/2 - 1$ and $N/2 + 1$. Then for a value of N , starting from values of $\beta = \epsilon\mu$ very small, and integrating the motion equations for times fairly long, we increase the value of β until the first pulse in the energy of the mode $N/2 - 1$ or, equivalently, the first sudden change in the energy of the mode $N/2$, appears. We assume this value of β as the value of β_t , the threshold energy density. In Fig. 28, the numerical value of β_t , determined in this way, and the theoretical value of β_t (formula (37)) are shown for $N = 4, 6, \dots, 64$.

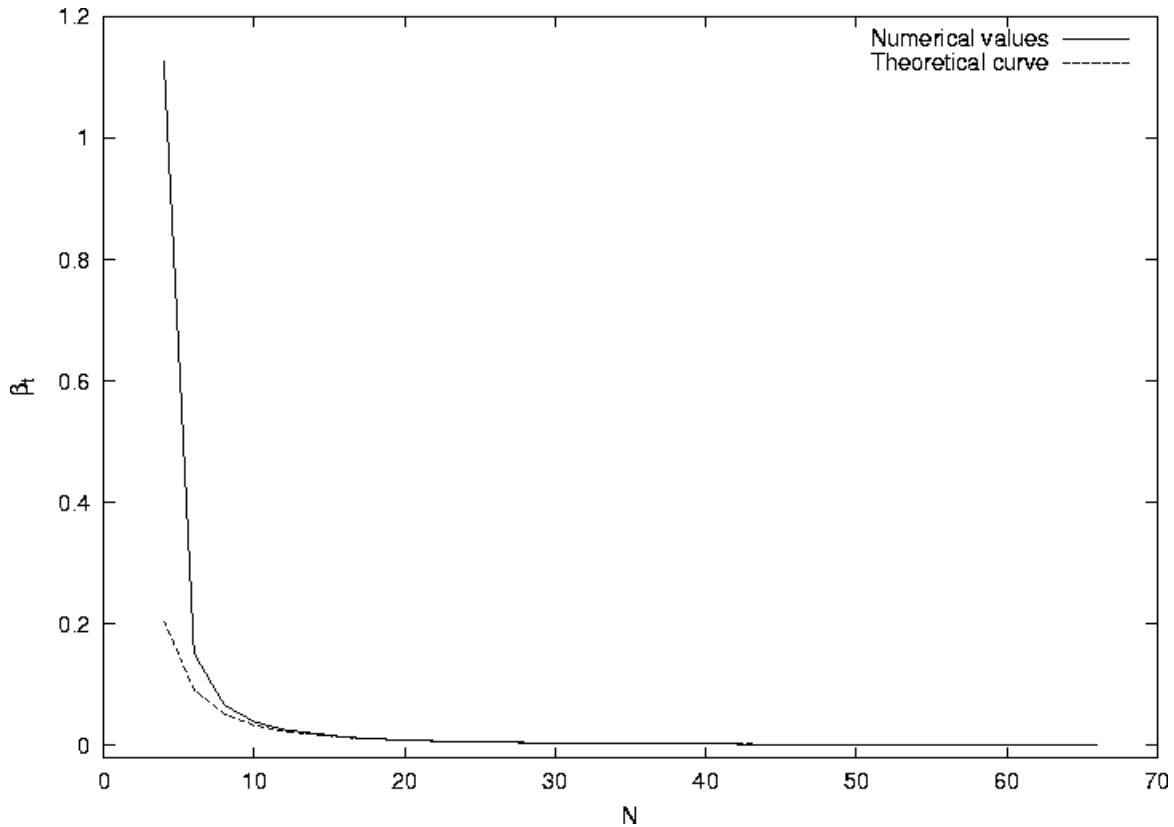


Figure 28: β_t vs N for the OMS $N/2$.

7 The cases $\frac{N}{4}$ and $\frac{3}{4}N$

Following the same procedure used in the case $N/2$, we have calculated, numerically, the threshold energy density for the two nonlinear OMS's $N/4$ and $(3/4)N$ as functions of N . We have found that β_t is the same in the two cases. In the case $N/4$, the initial condition $Q_{N/4} \neq 0$, $P_{N/4} = 0$ corresponds, in the variables q_k , to the initial configuration shown in Fig. 29.

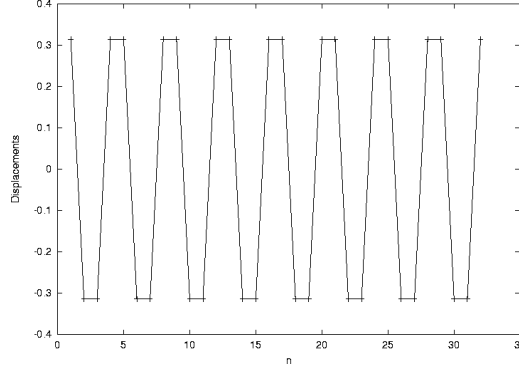


Figure 29: Initial configuration of the chain particles for the OMS $N/4$ for $N = 32$ and $\epsilon\mu = 0.01$. The displacements from the equilibrium positions are shown vs N .

We have found that the nonlinear OMS's $N/4$ and $(3/4)N$, for $N = 4$, $N = 8$ and $N = 12$, are stable in the limit of an integration time $T = 2 \times 10^4$.

The values of β_t , as a function of N , for the cases $N/2$ and $N/4$ are compared in Fig. 30:

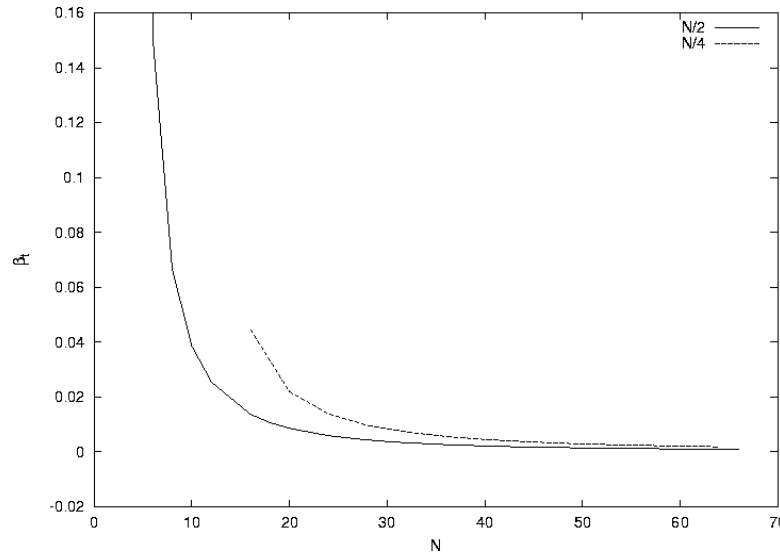


Figure 30: β_t vs N for the OMS's $N/2$ and $N/4$.

8 The case $N/3$ and $\frac{2}{3}N$

In this case, the initial condition: $Q_{N/3} \neq 0$, $P_{N/4} = 0$ corresponds, in the variables q_k , to the initial configuration shown in Fig. 31.

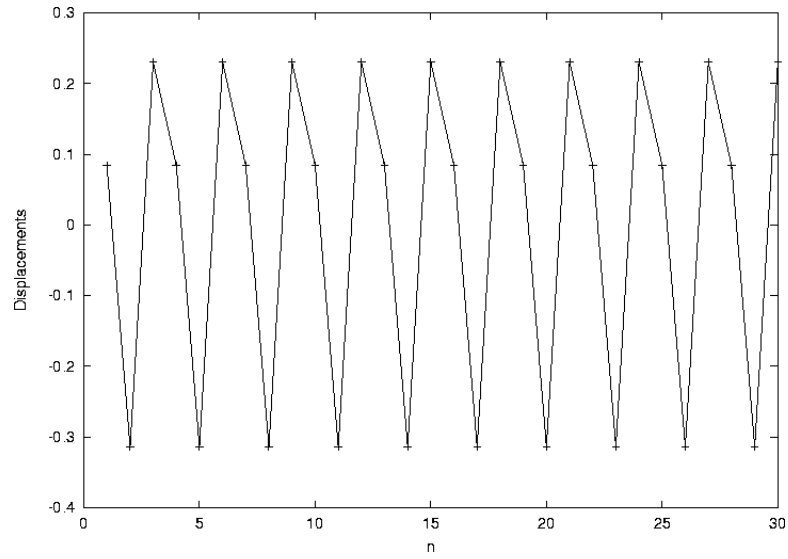


Figure 31: Initial configuration of the chain particles for the OMS $N/3$ for $N = 30$ and $\epsilon\mu = 0.008$. The displacements from the equilibrium positions, joined by segments, are shown vs N .

The behaviour of β_t , as a function of N , for the two cases, is given in the Fig. 32:

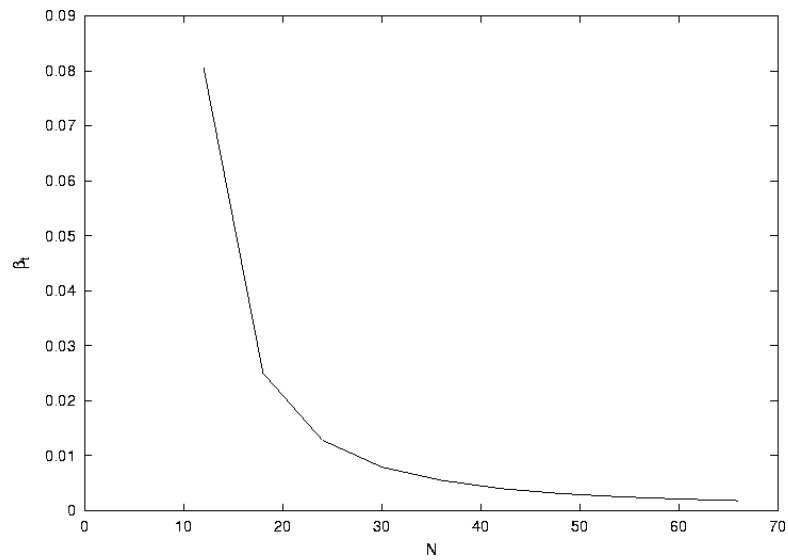


Figure 32: β_t vs N for the OMS's $N/3$ and $(2/3)N$

In the following table, for some even value of N between 4 and 64, the threshold β_t , for each OMS, is given.

N	$(\beta_t)_{\frac{N}{4}}$	$(\beta_t)_{\frac{N}{3}}$	$(\beta_t)_{\frac{N}{2}}$	$(\beta_t)_{\frac{1}{3}(\frac{\pi}{N})^2}$	$(\beta_t)_{\frac{3}{4}N}$	$(\beta_t)_{\frac{2}{3}N}$
4	stable		1.1272	0.2056	stable	
6		stable	0.1514	0.0914		stable
8	stable		0.0665	0.0514	stable	
10			0.0385	0.0329		
12	stable	0.0807	0.0254	0.0228	stable	0.0807
16	0.0447		0.0136	0.0128	0.0447	
18		0.0250	0.0106	0.0101		0.0250
20	0.0219		0.0086	0.0082	0.0219	
24	0.0138	0.0128	0.0059	0.0057	0.0138	0.0128
28	0.0096		0.0043	0.0042	0.0096	
30		0.0079	0.0037	0.0037		0.0079
32	0.0072		0.0033	0.0032	0.0072	
36	0.0056	0.0055	0.0026	0.0025	0.0056	0.0055
40	0.0045		0.0021	0.0021	0.0045	
42		0.0040	0.0019	0.0019		0.0040
44	0.0037		0.0018	0.0017	0.0037	
48	0.0031	0.0031	0.0015	0.0014	0.0031	0.0031
52	0.0027		0.0013	0.0012	0.0027	
54		0.0025	0.0012	0.0011		0.0025
56	0.0023		0.0011	0.0010	0.0023	
60	0.0021	0.0021	0.0010	0.0009	0.0021	0.0021
64	0.0018		0.0009	0.0008	0.0018	
66		0.0018	0.0009	0.0008		0.0018

The error is of one unit on the last digit.

In Fig. 33 the behaviour of β_t as a function of N is given for the cases $N/2$, $N/3$ and $N/4$. The first two values of β_t of the case $N/2$ have been left out for clarity.

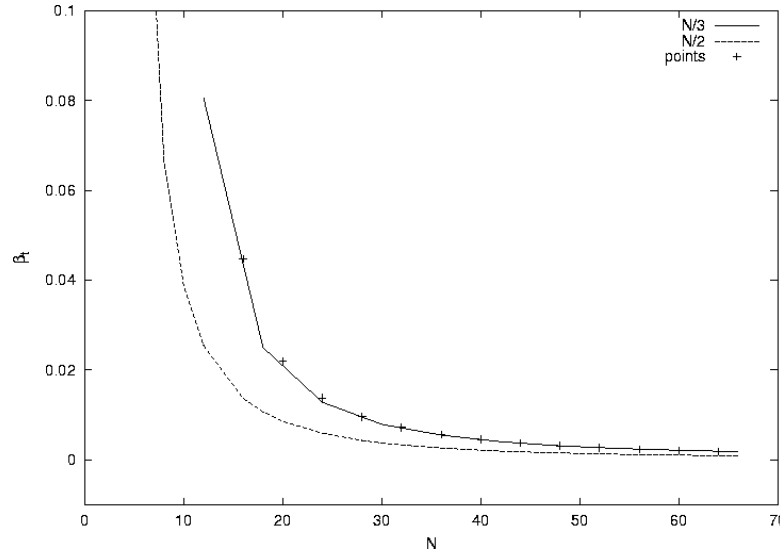


Figure 33: β_t vs N for the cases $N/2$, $N/3$ and $N/4$.

9 Discussion

We have numerically analyzed the stability of the OMS's in the Fermi-Pasta-Ulam system. Previously, only for the case $N/2$ were available theoretical analysis of the stability and approximate estimates of the stability threshold for large values of N . Our method is based on the numerical integration of full nonlinear differential equations of motion for the particles of the chain. The initial conditions for the hamiltonian variables q_k and p_k are such that only a particular nonlinear one-mode is initially excited. No a priori initial perturbation of the analytical solution is introduced in the numerical algorithm, the only perturbation being that generated by computational errors in numerical integration. Then the method studies the stability of the OMS's against the numerical errors introduced by the integration algorithm. We have widely analysed the case $N/2$, which in some sense works as a test, since, for this case, theoretical results are available.

We remark that the OMS's are nonlinear analytical solutions of the complete Fermi-Pasta-Ulam system, with linear and nonlinear terms in the hamiltonian, so their stability can't be discussed in terms of KAM theorem. The stability of linear modes and nonlinear OMS's, against computational errors, are completely disjoint in the sense that a linear mode, initially excited, is stable for very long integration times, if the parameter μ is set equal to zero in the hamiltonian. Thus the linear modes, excited during the evolution of a nonlinear OMS, are triggered by the instability of this nonlinear mode and then only indirectly by the computational errors. This is evident in Fig. 34, where the behaviour of energy vs time of the mode $N/2$ for $N = 32$, $\mu = 0.1$ and $\epsilon = 0.04$ is compared with the behaviour of the energy in the linear case with the same value of energy density $\epsilon = 0.04$ and $\mu = 0$.

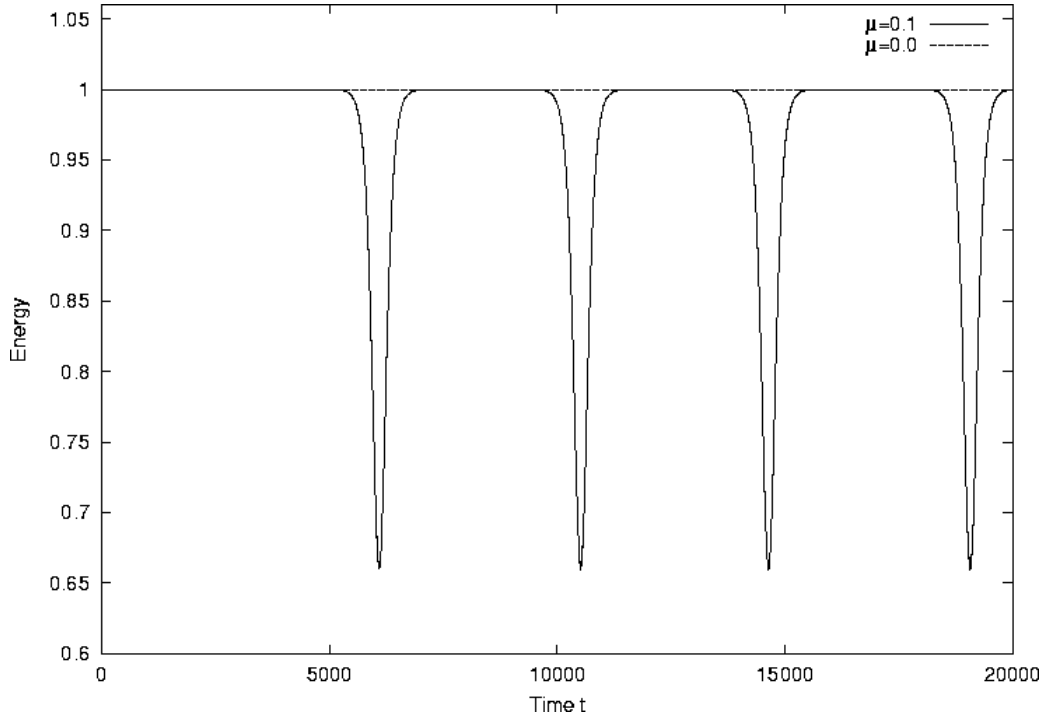


Figure 34: Energy as a function of time for $\epsilon = 0.04$ in the linear case $\mu = 0$, and $\mu = 0.1$.

As can be seen from this figure, the linear case is stable with respect to the computational errors of the numerical algorithm. This different behaviour of the linear mode and of the nonlinear OMS is much more evident if we compare, for the same integration time, the orbit in the plane $Q_{N/2}, P_{N/2}$, for the same value of $\epsilon = 0.5$ and the two values of $\mu = 0.0$, for the linear case, and $\mu = 0.5$ which corresponds, in the nonlinear case, to a value of β very much larger than the threshold value $\beta_t = 0.0033$. This different behaviour is shown in Fig. 35 and in Fig. 36.

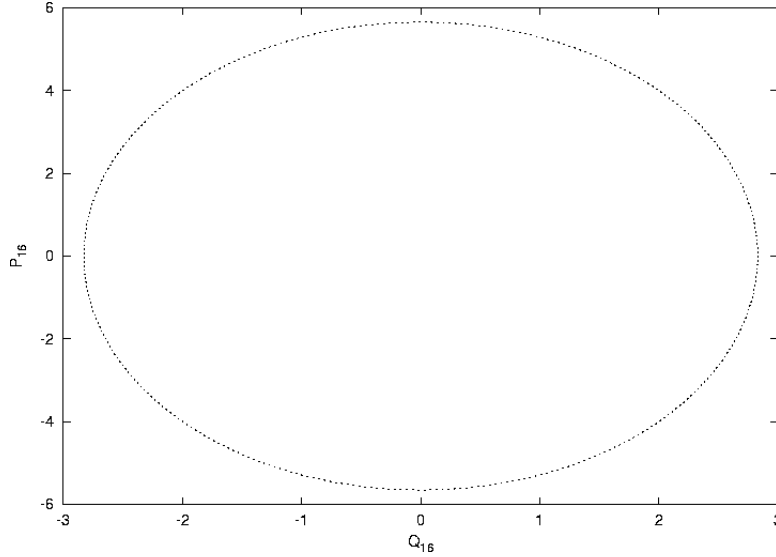


Figure 35: Orbit in the plane Q_{16}, P_{16} for the linear case ($\mu = 0$), with $\epsilon = 0.5$.

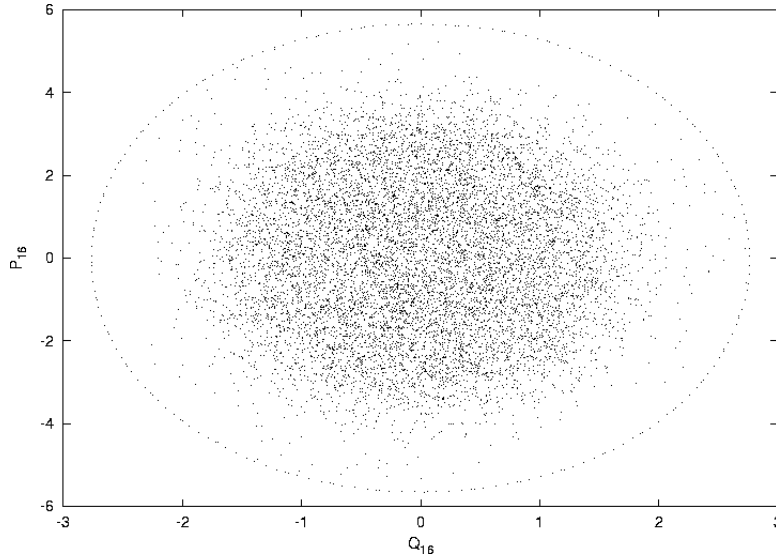


Figure 36: Orbit in the plane Q_{16}, P_{16} for the nonlinear case $\epsilon = 0.5, \mu = 0.1$.

Let us first consider the case $N/2$. From the inspection of Figs. 1 - 9, three regimes can be observed, varying the product $\beta = \epsilon\mu$. For values of β very small, well below the threshold energy density, the nonlinear OMS $N/2$ is stable and $Q_{N/2}$ is a periodic function with the same amplitude and the same period of the analytical solution (15). For values of β above and near the threshold, the situation is very different. The period of oscillation is equal to the period of the analytical solution, and for very long times, the representative point moves in the plane $Q_{N/2}, P_{N/2}$ on a one dimensional closed curve, as for very small values of $\epsilon\mu$; but now, periodically and for short times, the amplitude of oscillation varies, due to a decrease of modal energy, and the representative point of the system moves on an open curve which tends periodically to shrink. For $\epsilon\mu = 0.1$, well above the threshold energy density, we observe a chaotic behaviour.

In the first regime, where $\beta < \beta_t$, during the whole integration time, the OMS appears stable.

As soon as β exceeds β_t , after an initial time interval, depending on the precision of numerical calculations, during which the OMS is stable, the amplification of errors excites the first modes which become unstable, namely the modes $N/2 - 1$ and $N/2 + 1$. Because of the nonlinear coupling between the modes, the excitation of this two modes triggers all the other linear modes. The characteristics of this second regime, when the parameter β grows, are the increasing exchange of energy between the nonlinear mode and the other linear modes and the periodic recovery of energy of the nonlinear mode. This regime continues as long as the periodic exchange of energy is complete. Further increase of β , distorts the profile of the curve of energy of the nonlinear mode, as a function of time, and subsequently the system becomes chaotic.

We have seen that, for large values of N , formula (37) gives a good estimate of the instability threshold, so we could try to explain the "intermittent behaviour" of the second regime in the framework of the theory developed in [18]. As we have seen in section (4), modes with $\rho < 1/3$, are always stable in the linear approximation, for any energy density of the mode $n = N/2$, so that, perturbation of this mode, involving only modes with $\rho < 1/3$, never leads to instability. Let us consider for example the case $N = 32$. We have, from (32), that the modes with $r < 7$ are always stable in the linear approximation, for any energy density of mode $n = N/2 = 16$. These modes can grow only if they are triggered by the interaction with other unstable modes. As is pointed out in [18], this kind of interaction is neglected in the linear approximation and comes into play only when unstable modes have grown and the linearized theory is no longer valid. This indirect triggering is evident in the Figs. 37 - 38, where the time evolutions of the modes 16 and 6 are compared. No triggering of the mode 6 exists, if $\beta < \beta_t$.

For $\beta > \beta_t$, in the short time intervals, during which the nonlinear one-mode exchanges energy with the other modes, the time derivative of the energy of the OMS is not zero and the equation (14) and the formula (18) are no longer valid. During these time intervals, a strong coupling exists between the mode $N/2$ and the two adjacent modes and, indirectly, with all the other linear modes. However, the exact mechanism by which the nonlinear one-mode loses and recovers periodically energy is not clear. We try now to give an explanation of this mechanism in terms of Floquet's theorem for parametric oscillators [22], [23]. Let us consider the equation:

$$\frac{dx^2}{dt^2} + f(t)x = 0, \quad (39)$$

where $f(t)$ is a periodic function of time with period T . The Floquet's theorem means that the solution of (39) can be written in the form:

$$x_r(t) = \mu_r^{t/T} X_r(t), \quad (40)$$

where $r = 1$ or 2 , $\mu_1\mu_2 = 1$ and $X_r(t + T) = \pm X_r(t)$. The appropriate sign in front of $X_r(t)$ is determined by the particular form of $f(t)$. With the minus sign one has $X_r(t + 2T) = X_r(t)$. Solution (40) means also that

$$x_r(t + T) = \mu_r x_r(t). \quad (41)$$

Thus the values of $x_r(t)$, in successive cycles, increases by a factor μ when the time interval between the observations is equal to the period of $f(t)$. Concerning the stability of the oscillator, we can consider three separate cases ([24], [25]).

The first case corresponds to real values for both μ_1 and μ_2 . Since $\mu_1\mu_2 = 1$, one of them (e.g., μ_1) is greater than unity. After $N - 1$ cycles of oscillations, the magnitude of the displacement $|x_1(0)|$ grows to the value $|\mu_1|^N |x_1(0)|$ which exceeds $|x_1(0)|$: the

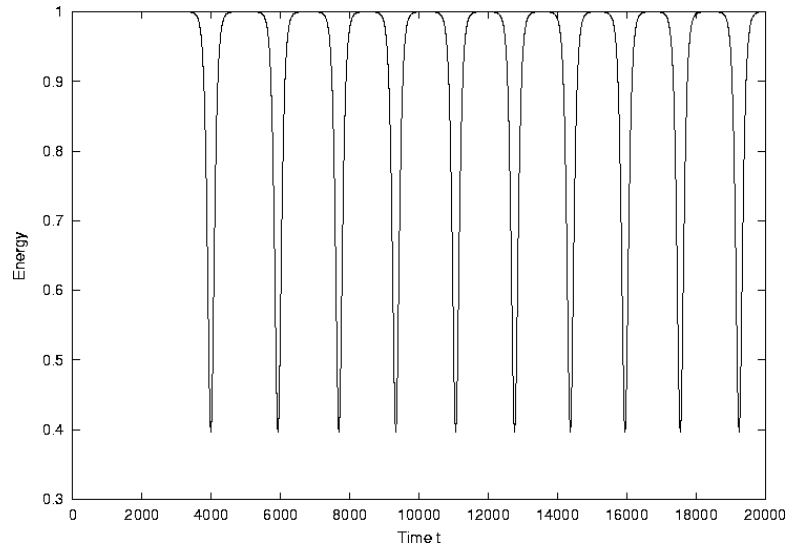


Figure 37: Energy of the mode 16 vs t for $\epsilon\mu = 0.005$.

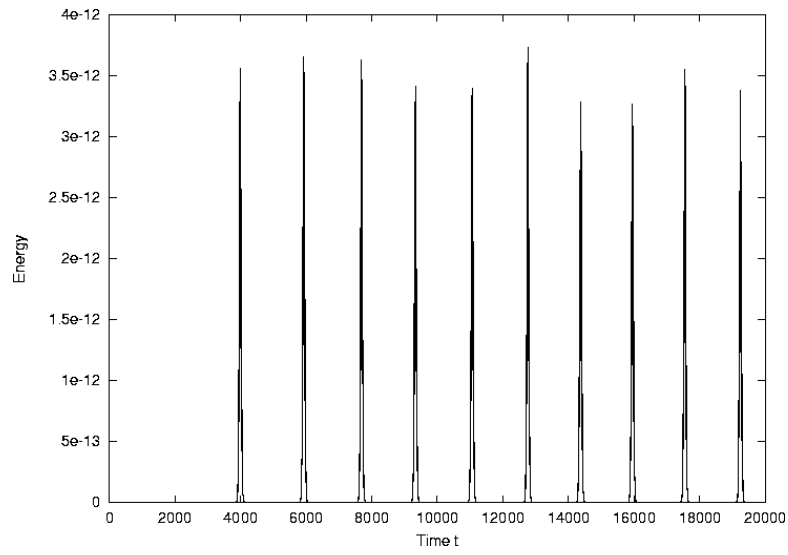


Figure 38: Energy of the mode 6 vs t for $\epsilon\mu = 0.005$.

displacement therefore diverges exponentially with N and the oscillations are unstable. The familiar case, known as "parametric resonance", occurs when $|\mu_1| > 1$ and the period of the Floquet function $X(t)$ is $2T$, where T is the period of $f(t)$.

The second case corresponds to $|\mu_1| = |\mu_2| = 1$. After $N - 1$ cycles of oscillation the size of the displacement is equal to the initial value, i.e., the oscillations are stable.

In the third case, $\mu_1^2 = \mu_2^2 = 1$, so that μ_1 and μ_2 have the same value and the case is "degenerate". In this case one can show that the degenerate oscillator is stable or unstable with displacement growing linearly with N .

In the matrix theory of the stability of eq. (39), μ_1 and μ_2 are roots of a quadratic equation. If we define the displacement and velocity at the beginning of the n -th cycle of the function $f(t)$ as x_n and v_n , respectively, the corresponding variables at the beginning of the next cycle of $f(t)$ are related to the vector $P(n) = (x_n, v_n)$ by two linear equations which can be written as the matrix equation

$$P(n+1) = M(T)P(n). \quad (42)$$

Thus the quadratic equation for μ is

$$\mu^2 - Tr[M(T)]\mu + Det[M(T)] = 0, \quad (43)$$

where $Tr[M(T)]$ and $Det[M(T)]$ are the trace and determinant of the 2×2 matrix $M(T)$ and $Det[M(T)] = \mu_1\mu_2 = 1$.

The matrix method is particularly useful in determining the stability of the solutions. Suppose that the graph of $f(t)$ vs t is approximated by a series of steps of width Δt and that the ordinate of the m -th step is ω_m^2 . With reference to our case, eq. (23), let us suppose $f(t) > 0$. The transformation matrix $[M(m)]$, relating the displacement $x(m+1)$ and velocity $v(m+1)$ at the end of the interval Δt_m to the respective values $x(m)$, $v(m)$ at the beginning, is obtained by solving the equation of motion, subject to the initial conditions $x = x(m)$ and $v = v(m)$. Since $f(t) = \omega_m^2$ is constant over the interval Δt_m , the equation of motion is that of a simple harmonic oscillator so that the following result is easily obtained:

$$M(m) = \begin{pmatrix} \cos(\omega_m \Delta t) & \sin(\omega_m \Delta t)/\omega_m \\ -\omega_m \sin(\omega_m \Delta t) & \cos(\omega_m \Delta t) \end{pmatrix}.$$

The complete transformation matrix $[M(T)]$, relating the initial and final column vectors, is obtained by taking the product of all the matrices for the entire time interval, i.e.:

$$M(t) = \prod M(m). \quad (44)$$

The question of stability is readily resolved by determining the eigenparameters of $M(T)$, that is to say, by solving a quadratic equation.

The pulsed behaviour of the energy of the nonlinear one-mode solution and the consequent pulsed behaviour of the linear modes can then be attributed to the time behaviour of the parameters μ_r , when $\beta > \beta_t$. Let us consider the Figs. 39 and 40 which show, for $N/2 = 16$ and $\beta = 0.005$, respectively the first energy pulse of the mode 15 and the correspondent time variation of Q_{15} .

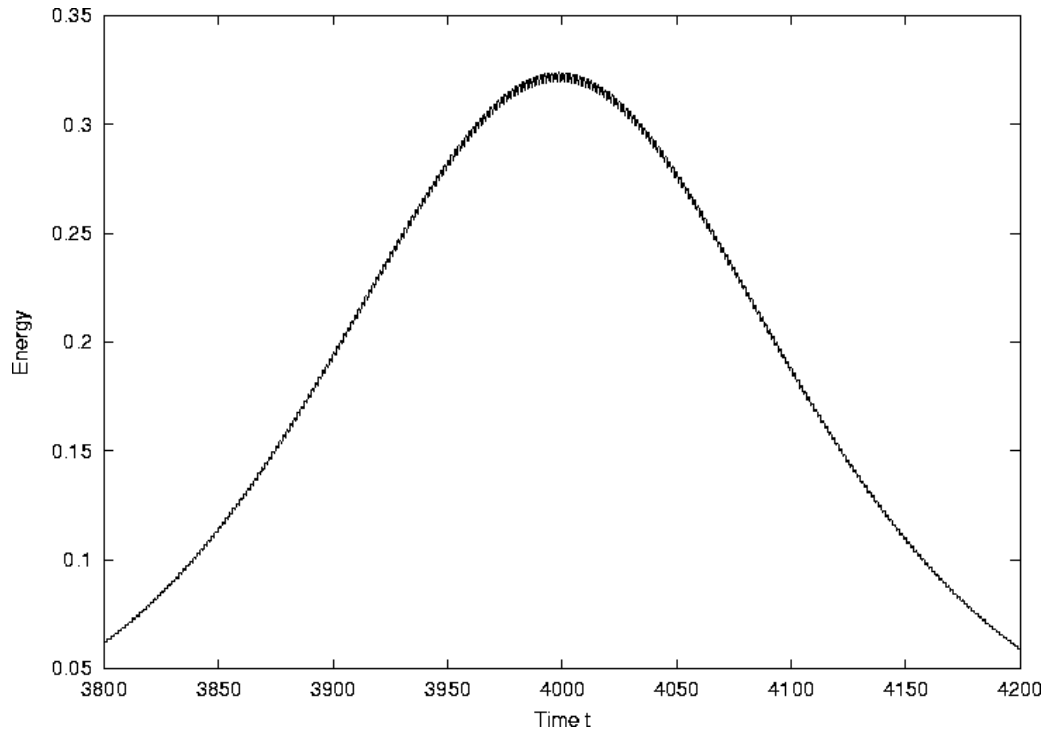


Figure 39: Energy of the mode 15 vs t for $\epsilon\mu = 0.005$.

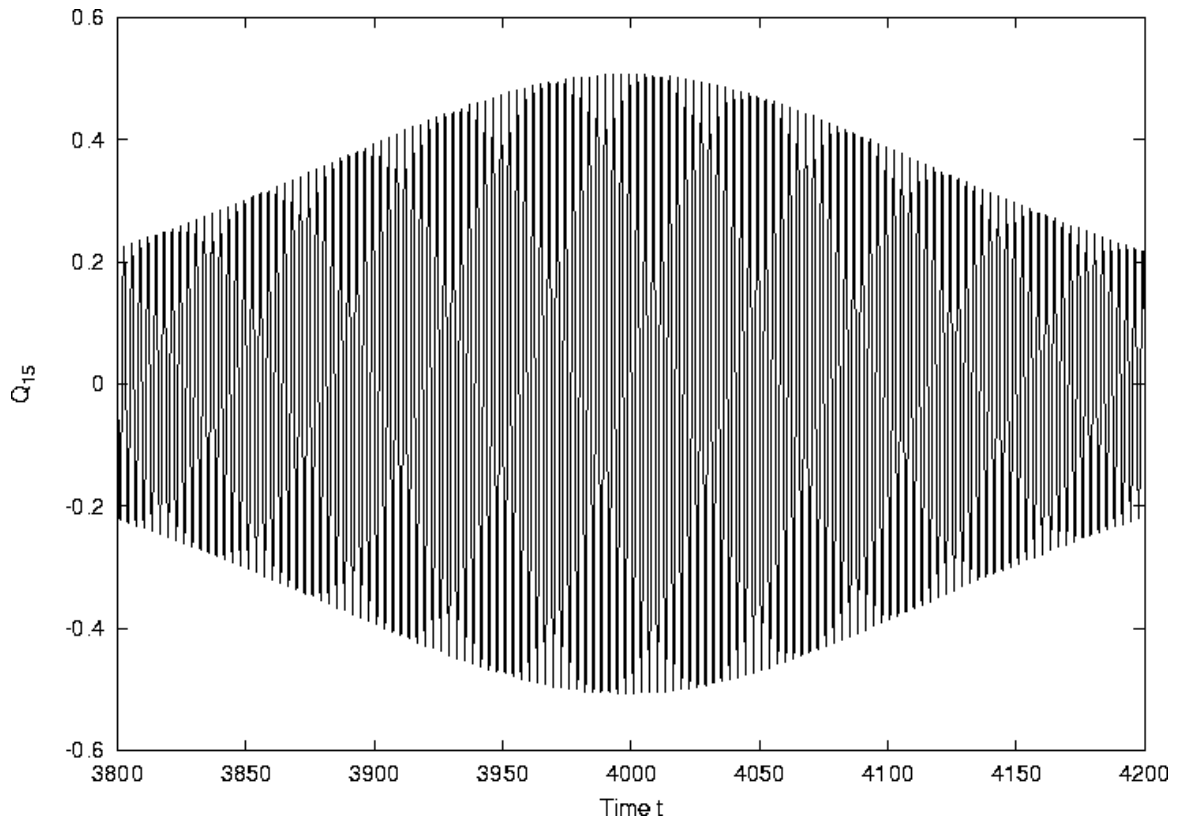


Figure 40: Q_{15} vs t for $\epsilon\mu = 0.005$.

From numerical data we have verified that, in our case, namely in the case of eq. (23), we have $X_r(t+T) = -X_r(t)$ and so $X_r(t+2T) = X_r(t)$, where T is the period of the Jacobian function $cn^2(\Omega_{N/2}t; k)$. For $\beta = 0.005$, from eqs. (16) and (17), we have $\Omega_{N/2} \approx \omega_{N/2}$ and $cn^2(\Omega_{N/2}t; k) \approx \cos^2 \omega_{N/2}t$. Since $\omega_{N/2} = 2$, the period of \cos^2 is $\pi/2$ and so $2T = \pi$. From eq. (41), comparing the values of Q_{15} each interval of $2T = \pi$, we can obtain the value of the parameter μ_r which determines the stability or instability of the solution. The pulsed behaviour of the solution and of the energy can then be attributed to a time variation of μ_r , due to the fact that, during the exchange of energy between the nonlinear one-mode and the other linear modes, eq. (23) is no longer exactly valid. If we suppose that the one-mode solution Q_{16} continues to oscillate with its normal frequency, but modulated in amplitude, during the energy exchange (see for example Fig. 5), then the parameter μ_r varies during this exchange, causing the typical pulsed behaviour for $\beta > \beta_t$. Obviously, if β is very large, many linear modes are involved, the exchange of energy is much greater and irreversible and the OMS does not recover all its initial energy: the whole system tends asymptotically to a state of energy equipartition. In figure 41 the time behaviour of the parameter μ is shown for the solution Q_{15} , when the one-mode excited is the one-mode $Q_{N/2}$, for $N = 32$ and $\beta = 0.005$. With reference to Fig. 40, the values of μ are obtained calculating the ratio between two consecutive maxima of Q_{15} . It is clear from Fig. 40 and Fig. 41 the link between the exponential growth and the

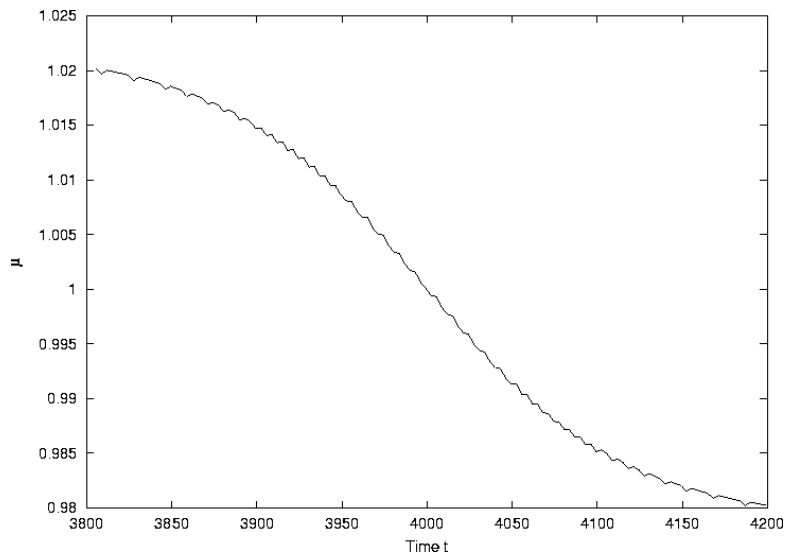


Figure 41: μ vs t for Q_{15} , $N = 32$ and $\epsilon\mu = 0.005$.

subsequent exponential decreasing of Q_{15} with the variation of the parameter μ from values greater than one to smaller values.

10 Conclusions

In this paper we have studied the problem of stability of the OMS's in the Fermi-Pasta-Ulam β oscillator chain. Although this problem has been tackled many times in the last years, analytical results were available only for the case $N/2$, where N is the number of particles in the chain. We have envisaged a simple numerical method, which tests the stability of solutions against the numerical errors introduced automatically by the numerical algorithm of integration of motion equations. The method reproduces the analytical results already known for case $N/2$, and

allows to obtain the threshold energy density above which the OMS is unstable, in the other cases, namely the cases $N/4$, $N/3$, $\frac{2}{3}N$ and $\frac{3}{4}N$.

We have found that, for each case, there is a characteristic energy density, above which, there is a large range of values of energy densities, before the chaotic region, in which the OMS presents an intermittent behaviour, in the sense that the nonlinear mode keeps its initial excitation energy for long times and periodically, abruptly, loses and recovers a fraction of this energy. We have verified that, for the case $N/2$, this characteristic energy density coincides, for large N , with the threshold energy density given by (22). Then we have assumed this characteristic energy density as threshold energy density also in the other cases.

We have also obtained that, varying N , the cases $\frac{N}{3}$, $\frac{2}{3}N$ and $\frac{N}{4}$, $\frac{3}{4}N$ have the same threshold energy density.

A tentative explanation of the intermittent behaviour, in terms of Floquet's theorem for parametric oscillators, has been given.

References

- [1] E. Fermi, J.R. Pasta and S. Ulam, Collected papers of E. Fermi, ed. E. Segre (University of Chicago, Chicago,1965).
- [2] J. Ford, J. Math. Phys. **2**, 387 (1961); J. Ford and J. Waters, J. Math. Phys., **4**, 1293 (1963).
- [3] E. A. Jackson, J. Math. Phys. **4**, 551 (1963).
- [4] R. S. Northcote and R. B. Potts, J. Math. Phys. **5**, 383 (1964).
- [5] F. M. Israiliev and B. V. Chirikov, Soviet Phys.-Doklady **11**, 30 (1966).
- [6] G. M. Zaslavsky and R. Z. Sagdeev, Soviet Phys.-JETP **25**, 718 (1967).
- [7] N. J. Zabusky, *Nonlinear Partial Differential Equations*, Academic Press, 1967, p. 223.
- [8] H. Poincaré, *Les Methodes Nouvelles de la Méchanique Celeste*, Blanchard, Paris, 1987, Vol. **3**, p. 389.
- [9] E. Fermi, Nuovo Cimento **25**, 267 (1923); **26** 105 (1923).
- [10] J. Ford, Phys. Rep. **213**, 271 (1992).
- [11] A. N. Kolmogorov, Dokl. Akad. Nauk SSSR **98**, 527 (1954); V. I. Arnold, Russ. Math. Surv. **18**, 9 (1963); J. Moser, Nachr. Akad. Wiss. Goettingen Math.-Phys. K1.2 1, 1 (1962).
- [12] N. Saito, N. Ooyama, Y. Aizawa and H. Hirooka, Suppl. of Prog. Theor. Phys. **45**, 209 (1970).
- [13] R. Livi, M. Pettini, S. Ruffo, M. Sparpaglione, A. Vulpiani, Phys. Rev. A **31**, 1039 (1985).
- [14] M. Pettini and M. Landolfi, Phys. Rev. A **41**, 768 (1990).
- [15] L. Casetti, M. Cerruti-Sola, M. Pettini and E. G. D. Cohen, Phys. Rev. E **55**, 6566 (1997).
- [16] H. Kantz, Physica D **39**, 322 (1989).
- [17] R. Livi, M. Pettini, S. Ruffo, M. Sparpaglione, A. Vulpiani, Phys. Rev. A **28**, 3544 (1983).
- [18] P. Poggi and S. Ruffo, Physica D **103**, 251 (1997).
- [19] N. Budinsky and T. Bountis, Physica D **8**, 445 (1983).
- [20] S. Flach, Physica D **91**, 223 (1996).
- [21] L. Casetti, Phys. Scripta **51**, 29 (1995).
- [22] L. D. Landau and E. M. Lifshitz, *Mechanics*, Pergamon, London, 1960.
- [23] N. Fameli, F. L. Curzon and S. Mikoshiba, Am. J. Phys. **67**, 127 (1999).
- [24] L. A. Pipes and L. R. Harvill, *Applied Mathematics for Engineers and Physicists*, Mc Graw - Hill, New York, 32nd ed., 1970.

[25] E. D. Yorke, Am. J. Phys. **46**, 285 (1978).